

## Many-electron multiplet effects in the spectra of 3d impurities in heteropolar semiconductors

A. Fazzio, M. J. Caldas, and Alex Zunger  
Solar Energy Research Institute, Golden, Colorado 80401  
(Received 16 March 1984)

The excitation energies of impurities in semiconductors, as well as their donor and acceptor ionization energies, represent a combination of one-electron and many-electron multiplet effects, where the latter contribution becomes increasingly significant as localized states are formed. Analysis of the absorption and ionization data for 3d impurities is often obscured by the inability of contemporary multiplet theories (e.g., the Tanabe-Sugano approach) to separate these two contributions and by the inadequacy of mean-field, one-electron theories that neglect multiplet effects altogether. We present a novel theory of the multiplet structure of localized impurities in semiconductors that circumvents the major shortcomings of the classical Tanabe-Sugano approach and at the same time separates many-electron from mean-field effects. Excitation and ionization energies are given as a sum of mean-field (MF) and multiplet corrections (MC):  $\Delta E = \Delta E_{MF} + \Delta E_{MC}$ . We determine  $\Delta E_{MC}$  from the analysis of the experimental data. This provides a way to compare experimentally deduced mean-field excitation and ionization energies  $\Delta E_{MF} = \Delta E - \Delta E_{MC}$  with the results of electronic-structure calculations. The three central quantities of the theory—the  $e$ - and  $t_2$ -orbital deformation parameters and the effective crystal-field splitting—can be obtained from mean-field electronic-structure calculations, or, alternatively, can be deduced from experiment. In this paper, we analyze the absorption spectra of 3d impurities in ZnO, ZnS, ZnSe, and GaP, as well as those of the bulk Mott insulators NiO, CoO, and MnO, in light of the new approach to multiplet effects. These mean-field parameters are shown to display simple chemical regularities with the impurity atomic number and the covalency of the host crystal; they combine, however, to produce interesting non-monotonic trends in the many-electron correction terms  $\Delta E_{MC}$ . These trends explain many of the hitherto puzzling discrepancies between one-electron ( $\Delta E_{MF}$ ) theory and experiment ( $\Delta E$ ). This approach unravels the chemical trends underlying the excitation and donor or acceptor spectra, provides predictions for unobserved excitations and donor or acceptor energies, and distinguishes the regime where one-electron theory is applicable ( $\Delta E_{MC}$  small) from the region where it is not ( $\Delta E_{MC} \sim \Delta E$ ).

### I. INTRODUCTION

The absorption spectra of transition-atom (TA) doped semiconductors show a series of rather sharp transitions at sub-band-gap energies (e.g., Refs. 1–20) that bear little resemblance to the single-particle excitations predicted by one-electron models (e.g., Refs. 21–29). For example, Fig. 1 depicts the absorption spectra of  $\text{Co}^{2+}$  impurity in a variety of tetrahedrally coordinated systems of varying covalency. Three well-resolved electronic transitions labeled in the figure,  ${}^4T_2$ ,  ${}^4T_1(F)$ , and  ${}^4T_1(P)$ , are observed with their attendant fine structure. One-electron models,<sup>21–23,26,29</sup> on the other hand, predict the existence of  $e$  and  $t$  impurity levels in the lowest quarter of the band gap (or even inside the valence band in GaP), assuming the configurations  $e^3t^3$  and  $e^4t^3$  in III-V and II-VI semiconductors, respectively. The excitation energies predicted by such models (e.g., in II-VI semiconductors  $e^4t^3 \rightarrow e^3t^4$  and  $e^4t^3 \rightarrow e^2t^5$ ) are at odds with experiment. The same is true for other 3d impurities. Table I provides a compilation<sup>3–19</sup> of some of the best-established  $d \rightarrow d^*$  transition energies for 3d impurities in ZnO, ZnS, ZnSe, and GaP. Attempts to correlate these transitions with differences in one-electron energy levels (or even with

total-energy differences) available in the literature<sup>21–29</sup> have met with little success. Similarly, the one-electron intraband  $d \rightarrow d^*$  excitations associated with the band structure<sup>30,31</sup> of Mott insulators such as bulk CoO and NiO (the stoichiometric limit of 3d impurities) bear little resemblance to the low-energy optical spectrum of these materials,<sup>32</sup> as band theory predicts these wide-band-gap insulators to be metals<sup>30–32</sup> (at least above the Néel temperature<sup>32</sup>).

Substantial discrepancies between theory and experiment also exist regarding the ordering of ionization energies<sup>1</sup> and the total spin of the ground-state wave functions determined by electron paramagnetic resonance (EPR).<sup>2</sup> The former problem is manifested in the data for the ionization spectra from the valence band (VB), e.g.,  $(\text{VB})^p t^n \rightarrow (\text{VB})^{p-1} t^{n+1}$  (single acceptors), and for the ionization spectra to the conduction band (CB), e.g.,  $(\text{CB})^0 t^n \rightarrow (\text{CB})^1 t^{n-1}$  (single donors). Table II [Refs. 3, 4, 6, 7, 10, 13, 14, 15(c), 17, and 33–46] provides a compilation of the most reliable donor and acceptor activation energies for TA impurities in GaP, ZnS, and ZnSe. These activation energies show a clear nonmonotonic trend with the impurity atomic number, with a local minimum at Mn and a maximum at Fe. In contrast, the calculated en-

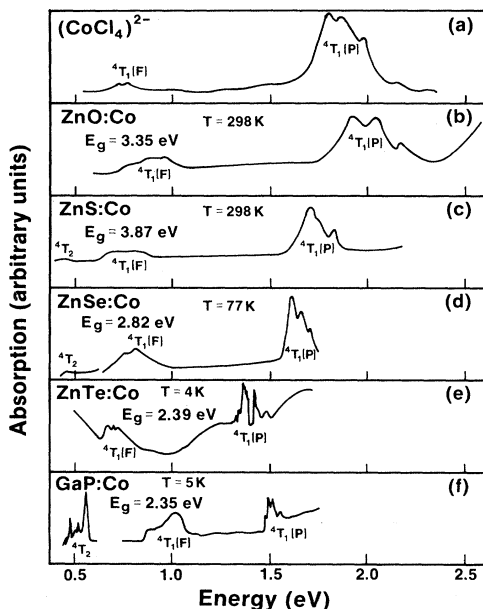


FIG. 1. Observed absorption spectra of the  $\text{Co}^{2+}$  impurity in tetrahedrally bonded semiconductors and in  $3d$  coordination compounds, drawn in the same energy scale, extracted from (a)  $(\text{CoCl}_4)^{2-}$ , Ref. 20; (b)  $\text{ZnO}:\text{Co}$ , Ref. 19; (c)  $\text{ZnS}:\text{Co}$ , Ref. 19; (d)  $\text{ZnSe}:\text{Co}$ , Ref. 12; (e)  $\text{ZnTe}:\text{Co}$ , Ref. 12; (f)  $\text{GaP}:\text{Co}$ , Ref. 14.

nergies of the one-electron impurity levels  $e$  and  $t_2$  show a clear monotonic decrease in binding energy with increasing atomic number.<sup>21–29</sup> The same monotonic trend persists in the calculated total-energy differences correspond-

ing to donor or acceptor transitions.<sup>21,22,26</sup> Furthermore, if one orders the various  $e^m t^n$  configurations calculated in one-electron theory<sup>25,26</sup> according to their total energies, one often finds that the predicted ground-state configuration corresponds to a low-spin state, whereas EPR data indicate a high-spin configuration (e.g., for a  $d^6$  impurity the calculated ground state corresponds to the configuration  $e^4 t^2$  with spin  $S=1$ , whereas the experimental ground state corresponds to the configuration  $e^3 t^3$  with  $S=2$ ). All of these discrepancies with experiment have long been suspected<sup>47–54</sup> to be related to many-electron multiplet effects left out of one-electron theory. Denoting by  $\hat{\mathcal{H}}_0$  the bare-ion Hamiltonian (i.e., that of a single unpaired electron, such as in  $\text{Fe}^{7+}$ ), by  $\hat{\mathcal{H}}_1$  the interelectronic interactions, and by  $\langle \hat{\mathcal{H}}_1 \rangle$  their mean-field average, one-electron theory in its standard space- and spin-restricted version [denoted here as the mean-field (MF) approach] provides solutions to the  $\hat{\mathcal{H}}_0 + \langle \hat{\mathcal{H}}_1 \rangle$  problem, leaving out the multiplet corrections (MC) that correspond to the  $\hat{\mathcal{H}}_1 - \langle \hat{\mathcal{H}}_1 \rangle$  problem. In one-electron MF theory, there is no place for the splitting between multiplets evident in the spectra of  $3d$  ions in solids (e.g., Fig 1). Although contemporary mean-field calculations do include average correlation effects in  $\langle \hat{\mathcal{H}}_1 \rangle$  (e.g., electron-gas correlation potentials in the local-density formalism), spatial correlations associated with the anisotropy of  $\hat{\mathcal{H}}_1 - \langle \hat{\mathcal{H}}_1 \rangle$  are excluded. In fact, band theory of simple metals and covalent semiconductors, as well as impurity theory of shallow defects, owe much of their success to the smallness of such multiplet effects in systems that sustain only extended and delocalized states. While it has

TABLE I. Observed excitation energies (in eV) in transition-atom-doped semiconductors used in this work for theoretical fitting of the spectra. The assignment of multiplet states is based on the present work.

Host	Ground state Impurity	${}^3A_2$ Ti	${}^4T_1$ V	${}^5T_2$ Cr	${}^6A_1$ Mn	${}^5E$ Fe	${}^4A_2$ Co	${}^3T_1$ Ni
ZnS			0.533 <sup>a</sup> ( ${}^4T_2$ )	0.645 <sup>b</sup> ( ${}^5E$ )	2.338 <sup>c</sup> ( ${}^4T_1$ )	0.442 <sup>d</sup> ( ${}^5T_2$ )	0.459 <sup>e</sup> ( ${}^4T_2$ )	0.543 <sup>g</sup> ( ${}^3T_2$ )
			1.141 <sup>a</sup> ( ${}^4A_2$ )	1.364 <sup>b</sup> ( ${}^3T_2$ )	2.529 <sup>c</sup> ( ${}^4T_2$ )	2.073 <sup>d</sup> ( ${}^3A_2$ )	0.769 <sup>e</sup> ( ${}^4T_1$ )	1.130 <sup>g</sup> ( ${}^3A_2$ )
			1.389 <sup>a</sup> ( ${}^4T_1$ )	1.748 <sup>b</sup> ( ${}^3T_1$ )	2.666 <sup>c</sup> ( ${}^4E$ )	2.138 <sup>d</sup> ( ${}^3A_1$ )	1.761 <sup>e,f</sup> ( ${}^4T_1$ )	1.536 <sup>g</sup> ( ${}^3T_1$ )
ZnSe		0.738 <sup>h</sup> ( ${}^3T_1$ )	0.500 <sup>a</sup> ( ${}^4T_2$ )	0.685 <sup>i</sup> ( ${}^5E$ )	2.309 <sup>j</sup> ( ${}^4T_1$ )	0.365 <sup>k</sup> ( ${}^5T_2$ )	0.434 <sup>l,k</sup> ( ${}^4T_2$ )	0.502 <sup>h</sup> ( ${}^3T_2$ )
		1.223 <sup>h</sup> ( ${}^3T_1$ )	1.085 <sup>a</sup> ( ${}^4A_2$ )	1.606 <sup>i</sup> ( ${}^3T_2$ )	2.467 <sup>j</sup> ( ${}^4T_2$ )	1.26 <sup>l</sup> ( ${}^3T_1$ )	0.781 <sup>l,k</sup> ( ${}^4T_1$ )	1.109 <sup>h</sup> ( ${}^3A_2$ )
			1.240 <sup>a</sup> ( ${}^4T_1$ )	1.853 <sup>i</sup> ( ${}^3T_1$ )	2.666 <sup>j</sup> ( ${}^4E$ )		1.674 <sup>l,k</sup> ( ${}^4T_1$ )	1.464 <sup>h</sup> ( ${}^3T_1$ )
GaP				0.873 <sup>m</sup> ( ${}^5E$ )	1.34 <sup>n</sup> ( ${}^4T_1$ )	0.413 <sup>o</sup> ( ${}^5T_2$ )	0.559 <sup>p</sup> ( ${}^4T_2$ )	0.583 <sup>q</sup> ( ${}^3T_2$ )
					1.53 (max)		1.051 <sup>p</sup> ( ${}^4T_1$ )	0.705 <sup>r</sup> ( ${}^3T_1$ )
							1.500 <sup>p</sup> ( ${}^4T_1$ )	1.240 <sup>r</sup> ( ${}^3T_1$ )
							1.426 <sup>r</sup> ( ${}^3A_2$ )	
ZnO							0.505 <sup>e</sup> ( ${}^4T_2$ )	
							0.843 <sup>e</sup> ( ${}^4T_1$ )	
							2.041 <sup>e</sup> ( ${}^4T_1$ )	

<sup>a</sup>Reference 3.

<sup>b</sup>Reference 4.

<sup>c</sup>Reference 5.

<sup>d</sup>References 6(a) and 6(b).

<sup>e</sup>Reference 19.

<sup>k</sup>Reference 12.

<sup>l</sup>Reference 13(a).

<sup>m</sup>Reference 15(a).

<sup>n</sup>Reference 16.

<sup>o</sup>Reference 17.

<sup>f</sup>Reference 7.

<sup>g</sup>Reference 8.

<sup>h</sup>Reference 9.

<sup>i</sup>Reference 10.

<sup>j</sup>Reference 11.

<sup>p</sup>Reference 14.

<sup>q</sup>Reference 15(b).

<sup>r</sup>Reference 18.

TABLE II. Observed single-acceptor (*A*), single-donor (*D*), and double-acceptor (*AA*) ionization energies in transition-atom-doped semiconductors. The energies are in eV, referred to the conduction- (*c*) band minimum or the valence- (*v*) band maximum, as indicated.

Host	Impurity	Sc	Ti	V	Cr	Mn	Fe	Co	Ni
ZnS	$E_c - 0.34^a (D)$	$\sim E_c - 1.74^b (D)$	$\sim E_c - 2.85^c (D)$ $E_v + 2.78^d (A)$	$E_c - (2.4 \pm 0.3)^e (D)$	In gap ( <i>D</i> )	In gap ( <i>D</i> )	$E_c - 2.46^f (A)$		
ZnSe	$E_c - 1.05^g (D)$	$E_c - 2.36^h (D)$ $E_v + 2.26^d (A)$	$\sim E_c - 1.55$ to $E_c - 1.7^i (D)$	$E_c - 2.64^k (D)$ $E_v + 1.85^f (A)$					
GaP		$E_v + 1.2^l (A)$	$E_v + (0.5 \pm 0.1)^m (D)$ $E_v + 1.12^n (A)$ $E_v + 1.85^o (AA)$	$E_v + 0.4^p (A)$	$E_c - 1.5^q (A)$ $E_c - 0.1^r (AA)$	$E_v + 0.41^s (A)$	$E_c - 0.5^t (A)$ $E_c - 0.8^u (AA)$		

<sup>a</sup>Reference 33, thermoluminescence.

<sup>b</sup>Reference 3, optical absorption, *n*-type sample grown from the melt in closed ampoule.

<sup>c</sup>Reference 4, photoconductivity.

<sup>d</sup>Reference 35, photo-EPR and optical absorption.

<sup>e</sup>A rather old value of  $E_c - 1.4$  eV was given by A. Rauber and J. Schneider [*Z. Naturforsch.* 17A, 266 (1962)]. Note, however, that Kodzheshpurov *et al.* [Ref. 6(b)] seem to have found the ZnS:Fe donor energy at  $\sim E_c - 2.4$  eV. This value is closer to that inferred in Ref. 6 (cf. Sec. VI C, i.e.,  $\sim E_c - 2.1$  eV. We hence use  $E_c - (2.4 \pm 0.3)$  eV.

<sup>f</sup>Reference 46, optical absorption.

<sup>g</sup>Reference 34, photoconductivity, crystal growth by vapor-phase epitaxy.

<sup>h</sup>Reference 10, optical absorption.

<sup>i</sup> $E_c - 1.55$  is a lower bound, estimated from Ref. 13(a), optically detected magnetic resonance by adding the shallow-donor energy ( $\sim 0.04$  eV) to the shallow-donor plus <sup>5</sup>*E* luminescence at 820 nm (1.51 eV). Optical-absorption data [Ref. 13(b)] suggests a value of  $\sim E_c - 1.7$  eV. We hence use the range  $E_c - 1.55$  to  $E_c - 1.7$ .

<sup>j</sup>Reference 44, photocapacitance.

<sup>k</sup>Reference 36, electroabsorption and cathodoluminescence.

<sup>l</sup>Reference 37, temperature dependence of conductivity, *n*-type sample grown by Czochralski method.

<sup>m</sup>Reference 15(c), optical quenching of EPR, *p*-type samples.

<sup>n</sup>Reference 38, photoluminescence.

<sup>o</sup>References 43(a) and 43(b).

<sup>p</sup>Reference 39, photoionization and temperature dependence of Hall constant, *n*-type samples grown by Czochralski method.

<sup>q</sup>Reference 40(a), quenching of EPR, *p*-type samples grown by Czochralski method [the value  $E_v + 0.78$  eV is given as the optical threshold in Ref. 40(b), whereas  $E_v + 0.82$  eV is the thermal enthalpy, close to  $E_v + 0.85$  eV given by Ref. 40(a)].

<sup>r</sup>Reference 45, EPR and temperature dependence of Hall constant, *n*-type samples grown from Ga solution.

<sup>s</sup>Reference 41, temperature dependence of Hall constant, *n*-type samples grown by vapor-phase epitaxy.

<sup>t</sup>Reference 42, ir absorption and temperature dependence of Hall constant, *n*- and *p*-type samples, grown by Czochralski method.

<sup>u</sup>Reference 14, excitation of luminescence, *n*-type samples.

been recognized on general grounds<sup>47–54</sup> that multiplet effects decrease in importance in going from localized excitations (e.g., in Mott-insulating  $3d$  oxides supporting localized magnetic moments or in  $3d$  impurities in insulators) to itinerant excitations (e.g., the metallic and weakly magnetic  $3d$  silicides<sup>55</sup> or  $sp$ -electron impurities in covalent semiconductors<sup>56,57</sup> such as Si:S and Si:Se), existing multiplet approaches have not separated multiplet effects from mean-field contributions as they have usually parametrized the  $\hat{\mathcal{H}}_0 + \hat{\mathcal{H}}_1$  problem directly. Indeed, contemporary approaches to the multiplet problem for impurities<sup>23,47–54</sup> have devised, with varying degrees of success, a number of phenomenological schemes for fitting the observed excitation spectra in terms of bare-ion energies (e.g., the “crystal-field parameter”  $\Delta_{\text{CF}} = \langle t | \hat{\mathcal{H}}_0 | t \rangle - \langle e | \hat{\mathcal{H}}_0 | e \rangle$ ) and the large perturbation to it associated with the full interelectronic repulsions underlying  $\hat{\mathcal{H}}_1$ . In treating the  $\hat{\mathcal{H}}_0 + \hat{\mathcal{H}}_1$  problem directly, these approaches have provided little help in establishing a connection with the results of MF electronic-structure calculations that treat the  $\hat{\mathcal{H}}_0 + \langle \hat{\mathcal{H}}_1 \rangle$  problem. The interplay between theory and experiment has often been obscured by statements on agreement or disagreement between the two (see, for example, the illuminating review of Ref. 32), when, in fact, the quantities extracted from experiment were not directly comparable with MF calculations.

In this paper we present an approach to the multiplet theory of impurities which separates MF from MC effects. We will seek to express the excitation or ionization energies  $\Delta E$  as a sum of a MF energy  $\Delta E_{\text{MF}}$  and the many-electron multiplet correction  $\Delta E_{\text{MC}}$ . Its three central quantities are the effective crystal-field energy  $\Delta_{\text{eff}}(m, n; m', n')$ , which separates the total MF energy of two one-electron configurations  $e^m t^n$  and  $e^{m'} t^{n'}$ , and the orbital deformation parameters  $\lambda_e$  and  $\lambda_t$ , which represent the ratio between the two-electron repulsion integrals in the solid and the free ion for the  $e$  and  $t_2$  representations, respectively (i.e., hybridization and covalency). These three quantities can be calculated from MF electronic-structure theory, or, alternatively, they can be deduced by fitting the observed excitation spectra. In the present work we determine them from the absorption spectra of all  $3d$  impurities in ZnO, ZnS, ZnSe, and GaP for which sufficient data are available (Table I), as well as for the bulk Mott insulators MnO, CoO, and NiO establishing the extent of MC underlying the data. Our analysis quantitatively isolates  $\Delta E_{\text{MC}}$  from  $\Delta E_{\text{MF}}$  in excitation and ionization, revealing the regular chemical trends (e.g., for donor or acceptor energies,  $\Delta E_{\text{MF}}$  is monotonic while  $\Delta E$  and  $\Delta E_{\text{MC}}$  are not), removes hitherto unexplained contradictions between MF calculations and experiments, and predicts the energy of some unobserved transitions.

## II. MEAN-FIELD ONE-ELECTRON APPROACH TO IMPURITIES

### A. Averaging the charge density

In electronic-structure calculations of systems with incomplete one-electron levels (e.g., open-shell ions, diatomic molecules such as  $\text{O}_2$ , bulk metals, Mott insulators,  $3d$

impurities, and core holes), one is constructing the one-body electronic charge density from the one-particle wave functions by a procedure equivalent to assuming equal populations of all partially filled degenerate spin orbitals. For example, if the sixfold-degenerate systems of a  $p$  shell in an atom, a  $t_2$  impurity level in a solid, or a  $\Gamma_{25}$  band in a crystal are to be occupied by two electrons, their contribution to the one-body charge density is calculated by means of a procedure equivalent to assigning  $\frac{2}{6}$  of an electron to each of the six degenerate partner levels. By Unsöld’s theorem this projection produces a totally symmetric  $a_1$  (spherically symmetric in free ions and atoms) charge density and one-body potential. (Although in muffin-tin<sup>21–25</sup> or other spherical approximations<sup>29</sup> this  $a_1$ -symmetric density is further approximated by a *spherically symmetric* density, this simplification is generally not necessary<sup>26–28</sup> and will not concern us here). The orbital energies obtained from the corresponding MF Schrödinger equation retain their original degeneracy (i.e., a self-consistent solution is obtained). These energies have in common a constant term (the Racah parameter  $A$ ) reflecting the interelectronic repulsion energy in this  $a_1$ -symmetric potential. While it is common to all degenerate partners, it is different for various space configurations [e.g., for impurities  $A(m, n) \neq A(m', n')$ ], reflecting variations in the spatial and angular extent of different self-consistent orbitals.

This spin- and space-restricted MF approximation constitutes an enormous computational simplification since different arrangements of electrons (e.g., excited states) experience potentials with the same ( $a_1$ ) symmetry, i.e., that underlying the nuclear framework. In crystals, this approach permits the use of Bloch-periodic, one-electron orbitals adapted to the symmetry of the *primitive* unit cell. While not mandated by any physical principle (only the *total* wave function must be Bloch-periodic), this approximation is nevertheless a computational panacea in band theory. At the same time, this approach deprives the system from gaining much of the spatial correlation energy since it does not allow different electron orbits to get out of each other’s way by occupying spatially distinct and variationally independent orbitals (e.g.,  $p_x$  and  $p_y$  in the  $p^2$  configuration, or different orbitals for different spins). This  $a_1$  symmetrization of the charge density is common to all MF contemporary approaches to the electronic structure of impurities.<sup>21–29,58–61</sup>

### B. Calculation of excitation and ionization energies in MF approaches

For the system of localized impurities that concerns us here, modern calculation techniques<sup>21–28,58,59</sup> allow accurate solutions for the self-consistent mean-field problem characterized by the sum of the bare-ion Hamiltonian

$$\hat{\mathcal{H}}_0 = -\frac{1}{2}\nabla^2 + V_{\text{ext}}^{\text{H}}(\vec{r}) + \Delta V_{\text{ext}}(\vec{r}) \quad (1)$$

and the  $a_1$ -averaged interelectronic Hamiltonian

$$\langle \hat{\mathcal{H}}_1 \rangle = V_{\text{scr}}^{\text{H}}(\vec{r}) + \Delta V_{\text{scr}}(\vec{r}) . \quad (2)$$

Here  $V_{\text{ext}}^{\text{H}}(\vec{r})$  and  $V_{\text{scr}}^{\text{H}}(\vec{r})$  represent the periodic host (H)

crystal external (ext) potential (e.g., pseudopotential) and screening (scr), respectively, whereas  $\Delta V_{\text{ext}}(\vec{r})$  and  $\Delta V_{\text{scr}}(\vec{r})$  denote the impurity-induced perturbations in the external potential and screening, respectively. Often,  $V_{\text{scr}}^{\text{H}}[\rho_{\text{H}}(\vec{r})]$  and  $\Delta V_{\text{scr}}[\rho_{\text{H}}(\vec{r}), \Delta\rho(\vec{r})]$  are calculated within the local-density formalism from the charge density  $\rho_{\text{H}}(\vec{r})$  of the host crystal and the impurity-induced density  $\Delta\rho(\vec{r})$ . Both  $\hat{\mathcal{H}}_0$  and  $\langle \hat{\mathcal{H}}_1 \rangle$  are restricted to the totally symmetric  $a_1$  representation of the impurity's point group (whether the lattice is relaxed or unrelaxed), although the corresponding impurity orbitals (as well as the sum of their squares) can belong to a lower-symmetry representation. Within this restriction, mean-field theories are able to produce excitation and ionization energies as differences in the corresponding total energies  $E_T$  (i.e., including orbital relaxation). For example, for a  $3d$  impurity on a cubic site sustaining  $e$  and  $t_2$  impurity-induced orbitals, the energy  $\Delta_{\text{eff}}(m, n; m', n')$  that separates two configurations is obtained as

$$\Delta_{\text{eff}}(m, n; m', n') = E_T(e^{m'} t^{n'}) - E_T(e^m t^n), \quad (3)$$

where the occupied VB is calculated self-consistently for each arrangement of electrons. This permits the calculation of MF excitation energies and the identification of the ground-state configuration by ordering  $\Delta_{\text{eff}}(m, n; m', n')$  for various configurations  $(m, n)$  and  $(m', n')$ . For  $sp$ -electron impurities such as Si:S and Si:Se, this approach<sup>56</sup> closely reproduces the observed excitation energies;<sup>57</sup> however, as we will see below, it fails completely for  $d$ -electron impurities. One can further calculate in mean-field theory the single-acceptor energy  $H_{\text{MF}}(-/0)$  relative to the valence band in the process where a neutral impurity  $A^0$  is transformed to a negatively charged impurity  $A^-$  by transference of a VB electron to a  $t$  level [hole ( $H$ ) emission],

$$H_{\text{MF}}^{(t)}(-/0) = E_T((\text{VB})^{p-1} t^{n+1}) - E_T((\text{VB})^p t^n), \quad (4)$$

or to an  $e$  level,

$$H_{\text{MF}}^{(e)}(-/0) = E_T((\text{VB})^{p-1} e^{m+1}) - E_T((\text{VB})^p e^m). \quad (5)$$

Analogous expressions exist for the single-donor energies relative to the conduction-band  $E_{\text{MF}}(0/+)$ , where  $A^0$  is transformed into a positively charged impurity  $A^+$  by transference of an  $e$  or a  $t_2$  electron to the conduction band (electron emission):

$$E_{\text{MF}}^{(t)}(0/+) = E_T((\text{CB})^1 t^{n-1}) - E_T((\text{CB})^0 t^n), \quad (6)$$

$$E_{\text{MF}}^{(e)}(0/+) = E_T((\text{CB})^1 e^{m-1}) - E_T((\text{CB})^0 e^m). \quad (7)$$

Acceptor transitions analogous to Eqs. (4) and (5) can also exist for transference of a conduction-band electron to the impurity (electron capture), and similarly, in an analogy with Eqs. (6) and (7), donor transitions can involve transference of a valence-band hole to the impurity (hole capture). For equilibrium transformations [pertinent to deep-level transient spectroscopy (DLTS) experiments], the total energies in Eqs. (4)–(7) are to be calculated for the lattice- and wave-function-relaxed systems, whereas for vertical (optical) excitations, the energy in Eq. (3) is to be calculated with wave-function relaxation, but for an

unrelaxed (i.e., ground-state) lattice geometry. In local-density calculations the transition-state approximation can be further used to obtain approximations to Eqs. (4)–(7) directly from the orbital energies  $\epsilon$ , e.g., for a  $t_2$  level,

$$H_{\text{MF}}^{(t)}(-/0) \simeq (\epsilon_t - \epsilon_{\text{VB}})_{(\text{VB})^{p-0.5} t^{n+0.5}}, \quad (8)$$

or

$$E_{\text{MF}}^{(t)}(0/+) \simeq (\epsilon_{\text{CB}} - \epsilon_t)_{(\text{CB})^{0.5} t^{n-0.5}}. \quad (9)$$

Variations in the orbital energies  $\epsilon(t^{n+0.5})$ , and  $\epsilon(e^{m+0.5})$ , or  $\epsilon(t^{n-0.5})$ , and  $\epsilon(e^{m-0.5})$ , with the impurity's atomic number, can thus be used to predict trends in the MF donor and acceptor energies, respectively. For  $sp$ -electron impurities, this approach reproduces the observed acceptor or donor energies;<sup>56–60</sup> however, as indicated below, it fails for the more localized  $d$ -electron impurities.

The Mott-Hubbard Coulomb repulsion energies  $U_{\text{MF}}^{(tt)}$  and  $U_{\text{MF}}^{(ee)}$  (the energy required to ionize an  $e$  or  $t$  electron, respectively, from a given site, and place the electron in a similar level on a distant site) can be obtained from the difference between the single-donor and single-acceptor energies (referred to the same band edge), e.g.,

$$U_{\text{MF}}^{(tt)} = E_{\text{MF}}^{(t)}(0/+) + H_{\text{MF}}^{(t)}(-/0) - E_g, \quad (10)$$

$$U_{\text{MF}}^{(ee)} = E_{\text{MF}}^{(e)}(0/+) + H_{\text{MF}}^{(e)}(-/0) - E_g,$$

where  $E_g$  is the energy gap, if the energies of the itinerant-host band edges remain unaffected by the addition or removal of a single electron. These Coulomb repulsion energies can be calculated in the transition-state approximation as

$$U_{\text{MF}}^{(tt)} \simeq \epsilon(t^{n+0.5}) - \epsilon(t^{n-0.5}), \quad (11)$$

$$U_{\text{MF}}^{(ee)} \simeq \epsilon(e^{m+0.5}) - \epsilon(e^{m-0.5}).$$

If lattice relaxation is absent, mean-field theory will always give  $U_{\text{MF}} > 0$  (i.e., donor excitation energy is below the acceptor excitation energy), since the difference in Eq. (11) represents the reduction in binding energy attendant upon increasing the occupation and hence interelectronic repulsions. Tight-binding approaches,<sup>61</sup> as well as other non-self-consistent methods that neglect occupation response, produce  $U_{\text{MF}} \equiv 0$ . Negative-effective- $U$  systems (i.e., acceptor below donor<sup>62</sup>) can exist if lattice relaxations stabilize the  $A^-$  system (relative to  $A^0$ ) more than they stabilize the  $A^+$  system. In the work of Masterov *et al.*,<sup>60(b)</sup>  $U_{\text{MF}}$  is viewed as a many-electron correction, although it is already present, as we have seen, in MF calculations. While it is first estimated<sup>60(b)</sup> from a simplified Hartree-Fock argument, it is then surprisingly argued that it should not be included in impurity calculations. All the results given<sup>60(b)</sup> hence pertain to bare (single-electron) impurity ions, a rather unphysical system.

If we now include multiplet effects as a correction to MF results, there is a correction  $\Delta E^{(i)}(m, n)$  to each many-electron multiplet  $i$  derived from the one-electron configuration  $(m, n)$ , which reflects the energy change associated with anisotropic electron repulsions  $\hat{\mathcal{H}}_1 - \langle \hat{\mathcal{H}}_1 \rangle$ .

The multiplet-corrected ground-state energy  $E_{(g.s.)}$  is now

$$E_{(g.s.)} = E_T(m^*, n^*) + \Delta E^{(i)}(m^*, n^*), \quad (12)$$

and hence the energy-minimizing configuration  $(m^*, n^*)$  can change relative to that obtained in MF theory. Owing to many-electron multiplet effects, the excitation energy between multiplets  $|i\rangle$  and  $|j\rangle$  of Eq. (3) is replaced by the excitation energy

$$E_{exc} = \Delta_{eff}(m, n; m', n') + [\Delta E^{(j)}(m', n') - \Delta E^{(i)}(m, n)]. \quad (13)$$

The single-acceptor energy of Eqs. (4) and (5) changes to

$$\begin{aligned} H^{(\mu)}(-/0) &= H_{MF}^{(\mu)}(-/0) + [\Delta E^{(j)}(A^-) - \Delta E^{(i)}(A^0)], \\ &\equiv H_{MF}^{(\mu)}(-/0) + \Delta H(-/0), \end{aligned} \quad (14)$$

where  $\Delta E^{(j)}(A^-)$  and  $\Delta E^{(i)}(A^0)$  are the multiplet corrections to the ground state  $|j\rangle$  of  $A^-$  and the ground state  $|i\rangle$  of  $A^0$ , and  $\mu$  stands for  $e$  or  $t_2$ . The donor energy of Eqs. (6) and (7) changes, correspondingly, to

$$\begin{aligned} E^{(\mu)}(0/+ ) &= E_{MF}^{(\mu)}(0/+ ) + [\Delta E^{(k)}(A^+) - \Delta E^{(l)}(A^0)] \\ &\equiv E_{MF}^{(\mu)}(0/+ ) + \Delta E(0/+ ), \end{aligned} \quad (15)$$

and the Coulomb energies of Eq. (10) are replaced by

$$\begin{aligned} U^{(\mu\mu)} &= U_{MF}^{(\mu\mu)} + [\Delta E(0/+ ) + \Delta H(-/0)] \\ &\equiv U_{MF}^{(\mu\mu)} + \Delta U^{(\mu\mu)}. \end{aligned} \quad (16)$$

The significance of the many-electron correction terms in Eqs. (12)–(16) can be assessed by comparing the results of contemporary MF calculations<sup>21–29</sup> to experiment. The situation can be summarized as follows: (i) Ordering the MF total energies for various impurity configurations incorrectly predicts low-spin ground-state configurations for the  $d^2$  to  $d^6$  substitutional impurities in Si, GaAs, and GaP, in contrast to the high-spin configuration evident from EPR studies<sup>2</sup> [viz., the  $\Delta E^{(i)}(m, n)$  correction of Eq. (12)]. (ii) Calculated  $d \rightarrow d^*$  excitation energies are too small for all but the lowest-lying transitions [viz., the correction term in square brackets in Eq. (13)]. This is true both for  $3d$  impurities and the intraband transitions in  $3d$  oxides.<sup>30,31</sup> (iii) MF theory predicts for unrelaxed impurities a monotonic decrease in donor energies and a similarly monotonic increase in acceptor energies as the impurity's atomic number varies from Ni to V, whereas experiment (cf. Table II) exhibits a clear, nonmonotonic behavior in both cases [viz., the corrections  $\Delta H(-/0)$  and  $\Delta E(0/+)$  in Eqs. (14) and (15)]. For instance, in III-V semiconductors the observed Mn single-acceptor state is always lower in energy than that of Fe, whereas the calculated MF levels<sup>21–23,26,29</sup> of Mn are higher than those of Fe. Note that these discrepancies in trends could be identified only because both experiments and theory were performed on series of impurities. We note that all of these discrepancies appear to be considerably smaller for  $sp$ -bonded impurities such as Si:S and Si:Se,<sup>56</sup> or the antisite defect in GaAs,<sup>60</sup> for which excellent agreement exists between recent MF calculations and experiment.

Our objective here is to develop an approach that would enable us to separate multiplet corrections from MF effects as in Eqs. (12)–(16), providing guides to the success

and failures of electronic-structure calculations on localized impurities and clarifying the chemical trends in the many-electron corrections. We first review the traditional approach to the problem.

### III. CONTEMPORARY MULTIPLY APPROACHES

Whereas the spin- and space-restricted mean-field approach distributes  $N$  electrons in a single fixed way in  $M$ -fold-degenerate spin orbitals ( $N/M$  electrons in each), there are  $\binom{M}{N}$  distinct ways (one for closed-shell systems) to do this. These  $\binom{M}{N}$ -independent Slater determinants represent charge densities with symmetries equal to or lower ("broken symmetries") than the totally symmetric  $a_1$  representation underlying the nuclear framework. Whereas they belong to the same eigenvalue, they may have different total energies, as both the interelectronic repulsion and the exchange interactions depend on the orientation of the occupied orbitals. These determinantal states can couple through interelectronic interactions to form new combination states  $i = {}^{2S+1}\Gamma$  (multiplets of spin  $S$  and space symmetry  $\Gamma$ ) having the correct global symmetry mandated by the point group, total spin, and orbital momentum. In standard multiplet approaches<sup>47–53</sup> one is tacitly assuming that there exists a small subset of one-electron orbitals (e.g.,  $e$  and  $t_2$  orbitals for  $d$ -electron impurities on cubic sites) that carry the multiplet corrections; the coupling channel to the entire system is included implicitly, as the MF energies of these orbitals depend on the occupation and screening exerted by all other relevant states (e.g., valence-band resonances). The  $\alpha$ th diagonal element of the  $\hat{\mathcal{H}}_0 + \hat{\mathcal{H}}_1$  matrix in this determinantal basis is given for the  $\Gamma$ th representation as

$$\Gamma D_{\alpha\alpha}(m, n) = E_{SC}^{\alpha}(m, n) + k_{\alpha\alpha} \Delta_{CF}, \quad (17)$$

where the single-configuration (SC) energy  $E_{SC}^{\alpha}(m, n)$  is the matrix element of  $\hat{\mathcal{H}}_1$  and the crystal-field parameter  $\Delta_{CF}$  is the difference in diagonal elements of the bare-ion Hamiltonian  $\hat{\mathcal{H}}_0$  taken with respect to the partner states  $\phi_1, \dots, \phi_6$  of the  $t_2$  representation and the partner states  $\phi_7, \dots, \phi_{10}$  of the  $e$  representation:

$$\Delta_{CF} = \langle \phi_t | \hat{\mathcal{H}}_0 | \phi_t \rangle - \langle \phi_e | \hat{\mathcal{H}}_0 | \phi_e \rangle. \quad (18)$$

The numerical factor  $k_{\alpha\alpha}$  in Eq. (17) arises from the fact that the diagonal elements are taken with respect to a fixed configuration [often,<sup>47,48,51</sup>  $k_{\alpha\alpha} \Delta_{CF}$  is replaced by  $(6m - 4n)Dq$  where "10Dq" is the crystal-field parameter in the point-charge model]. Using  $e^m t^n$  with  $m + n = 2$  as an example, the  ${}^3T_1$  multiplet arising from the configurations  $e^0 t^2$  and  $e^1 t^1$  gives rise to a  $2 \times 2$  matrix with diagonal elements ( ${}^{2S+1}\Gamma = {}^3T_1$ ):

$$D_{11}(e^0 t^2) = \langle t^2 | \hat{\mathcal{H}}_1 | t^2 \rangle + 2 \langle \phi_t | \hat{\mathcal{H}}_0 | \phi_t \rangle \quad (19)$$

and

$$\begin{aligned} D_{22}(e^1 t^1) &= \langle e^1 t^1 | \hat{\mathcal{H}}_1 | e^1 t^1 \rangle + \langle \phi_t | \hat{\mathcal{H}}_0 | \phi_t \rangle \\ &\quad + \langle \phi_e | \hat{\mathcal{H}}_0 | \phi_e \rangle. \end{aligned}$$

When referred to the bare energy of the configuration  $e^2 t^0$ , one subtracts from the diagonal elements of Eq. (19)

the term  $2\langle\phi_e|\hat{\mathcal{H}}_0|\phi_e\rangle$  pertinent to this reference configuration, yielding

$$\begin{aligned} D_{11}(e^0t^2) &= \langle t^2 | \hat{\mathcal{H}}_1 | t^2 \rangle + 2\Delta_{\text{CF}}, \\ D_{22}(e^1t^1) &= \langle e^1t^1 | \hat{\mathcal{H}}_1 | e^1t^1 \rangle + \Delta_{\text{CF}}, \end{aligned} \quad (20)$$

and hence in Eq. (17)  $k_{11}=2$  and  $k_{22}=1$ . The off-diagonal elements of the interaction matrix represent configuration mixing (CM) between two configurations,  $(m,n)$  and  $(m',n')$ , that belong to the same multiplet, given as

$$\Gamma D_{\alpha\beta} = E_{\text{CM}}^{\alpha\beta}(m,n;m',n'). \quad (21)$$

For the  ${}^3T_1$  multiplet, we have

$$D_{12} = \langle t^2 | \hat{\mathcal{H}}_1 | e^1t^1 \rangle \quad (22)$$

and

$$D_{21} = \langle e^1t^1 | \hat{\mathcal{H}}_1 | t^2 \rangle.$$

If the partner orbitals  $\phi_1, \dots, \phi_{10}$  are taken as general bases that span the representation  $e$  and  $t_2$  of the system's point group, the elements  $E_{\text{SC}}^e$  and  $E_{\text{CM}}^{\alpha\beta}$  are specified by 10 independent interelectronic integrals<sup>53</sup> (Slater-Condon integrals) of the form  $\langle\phi_i\phi_j|1/r_{12}|\phi_k\phi_l\rangle$ . While these can be calculated in a straightforward manner from the impurity orbitals (the calculation is particularly easy when single-site orbitals are used<sup>63</sup>), such a 10-parameter problem is not well suited for comparison with experiment as typically only 2–4 transitions are observed (cf. Table I). If, on the other hand, it is assumed that the  $e$  and  $t_2$  orbitals share the same radial part and each have a single Kubic harmonic with  $l=2$ , these 10 integrals collapse to three independent ones, denoted as the Racah parameters  $A$ ,  $B$ , and  $C$ , where  $A$  corresponds to the  $a_1$ -symmetric part of the electron repulsion, and  $B$  and  $C$  correspond to anisotropic interactions.<sup>47,48</sup> This is, in fact, a rather drastic approximation since modern mean-field calculations<sup>21–29</sup> reveal that the hybridization with host orbitals, orthogonality at ligand sites, and screening by the host states lead to distinctly different radial functions for  $e$  and  $t_2$  orbitals. This approximation of neglecting “differential hybridization”<sup>47</sup> of  $e$  relative to  $t_2$  can be improved<sup>23,49,50</sup> by scaling the group integrals  $A$ ,  $B$ , and  $C$  by the orbital deformation parameters  $\lambda_e$  and  $\lambda_t$ , reflecting the ratio between interelectronic repulsions in the solid (sol) and the free ion (ion):

$$\lambda_e^4 = \frac{\langle ee || ee \rangle_{\text{sol}}}{\langle dd || dd \rangle_{\text{ion}}}, \quad \lambda_t^4 = \frac{\langle tt || tt \rangle_{\text{sol}}}{\langle dd || dd \rangle_{\text{ion}}}. \quad (23)$$

These integrals can be evaluated from mean-field electronic-structure calculations using the  $l=2$  projection of the fully hybridized, self-consistent orbitals. The mixed deformation parameter  $\lambda_{et}$  can be calculated in analogy with Eq. (23), or estimated<sup>23,48</sup> as  $\lambda_{et} = (\lambda_e\lambda_t)^{1/2}$ . In this approach, the single-configuration energy  $E_{\text{SC}}(\lambda_e, \lambda_t, A, B, C)$  depends also on  $A$ , whereas the configuration mixing  $E_{\text{CM}}(\lambda_e, \lambda_t, B, C)$  does not. For the  ${}^3T_1$  multiplet used as an example, we have

$$D_{11}(e^0t^2) = \lambda_t^4 A(0,2) - 5\lambda_t^4 B + 2\Delta_{\text{CF}}, \quad (24)$$

$$D_{22}(e^1t^1) = \lambda_e^2 \lambda_t^2 A(1,1) + 4B\lambda_e^2 \lambda_t^2 + \Delta_{\text{CF}},$$

whereas the off-diagonal configuration mixing is given as

$$D_{12}(e^0t^2; e^1t^1) = -6B\lambda_e\lambda_t^3. \quad (25)$$

Here we have used the notation  $A(m,n)$  to emphasize the configuration dependence of the  $a_1$ -symmetric interelectronic repulsion energy.

Expressions (17)–(25) can be used to discuss the properties of a few contemporary multiplet approaches. In the atomic (Racah's) limit (e.g., discussion in Ref. 47), the  $e$  and  $t_2$  orbitals unite to form the free-ion  $d$  orbital; hence  $\Delta_{\text{CF}}=0$ ,  $\lambda_e=\lambda_t=1$ , and  $A(N)$  appears identically in all diagonal terms and as such does not affect the multiplet splitting. The observed transitions can be fitted in terms of  $B$  and  $C$ , yielding the free-ion values  $B_0$  and  $C_0$  collected in Ref. 47.

In the classical Tanabe-Sugano-Kamimura treatment<sup>48</sup> for ions in solids, differential hybridization is neglected ( $\lambda_e=\lambda_t$ ). The multiplet energies should still depend on  $A(m,n)$ ; since  $A$  is by far the largest of all interaction integrals [ $A \approx (10-100)B$ ;  $C \approx 4B$ ], even a weak dependence on  $(m,n)$  can alter the results significantly. Nevertheless, in analogy with the free-ion case, the configuration dependence of  $A$  has been neglected in this approach<sup>48</sup> (the configuration dependence of  $B$  and  $C$  is negligibly small), leading to a common  $A$  in all diagonal elements. The observed transitions are then fitted to  $B$ ,  $C$ , and  $\Delta_{\text{CF}}$  (hence the term the “ $B$ ,  $C$ , and  $\Delta_{\text{CF}}$  approach”). Since  $\Delta_{\text{CF}}$  is configuration independent, this approach does not provide a channel for coupling the impurity orbitals to the host crystal. This approach, the cornerstone of numerous applications in the past 30 years (e.g., see the reviews in Refs. 20, 47, 48, 51, and 54), has led to many successful interpretations of spectra. At the same time, it has not been free of difficulties. First, if the number of observed transitions exceeds the number of parameters, the unfitted transitions are often poorly predicted (see the discussion in Ref. 53). Second, the results of the fit do not lend themselves to clear comparisons with electronic-structure studies, because implicit in the latter are the configuration dependence of  $A$  and differential hybridization, which are neglected in the  $B$ ,  $C$ , and  $\Delta_{\text{CF}}$  approach. Indeed, the chemical trends in the fitted  $\Delta_{\text{CF}}$  (e.g., the  $S$ -shaped curve for  $3d$  impurities in II-VI semiconductors<sup>12</sup>) are rarely matched by state-of-the-art electronic-structure calculations. Third, accidental degeneracies are predicted by the fit that do not seem to exist in the data.<sup>53</sup>

The Hemstreet-Dimmock (HD) approach<sup>23</sup> [see also Refs. 21(b), 25, and 28] represents a pioneering attempt to bridge the classical  $B$ ,  $C$ , and  $\Delta_{\text{CF}}$  approach with the content of electronic-structure calculations. First, differential hybridization is introduced through the orbital deformation parameters  $\lambda$ , e.g., the ratio between two interelectronic repulsion integrals,

$$\lambda_e^4 = \int_0^\infty \int_0^\infty \phi_e(r_1)\phi_e^*(r_2) \frac{r_1^k}{r_1^{k+1}} \phi_e(r_1)\phi_e^*(r_2) dr_1 dr_2 / \int_0^\infty \int_0^\infty \phi_d(r_1)\phi_d^*(r_2) \frac{r_1^k}{r_1^{k+1}} \phi_d(r_1)\phi_d^*(r_2) dr_1 dr_2, \quad (26)$$

that are, however, replaced by the square of the fraction of  $l=2$  charge enclosed in a sphere of radius  $R_{\text{MT}}$ ,

$$\tilde{\lambda}_e^4 = \left[ \int_0^{R_{\text{MT}}} \phi_e(r) \phi_e^*(r) r^2 dr / \int_0^\infty \phi_d(r) \phi_d^*(r) r^2 dr \right]^2, \quad (27)$$

where  $R_{\text{MT}}$  is the muffin-tin (MT) radius (usually half of the bond length of the host crystal). While intuitively appealing, it is not obvious whether Eq. (27) forms a reasonable approximation to Eq. (26) since the interelectronic operator of Eq. (26) (sensitive to small  $r_1$ - $r_2$  regions) is replaced by unity in Eq. (27) (weighing all space equally). Second, the *bare-ion* parameter  $\Delta_{\text{CF}}$  is replaced by the  $t-e$  eigenvalue difference from a mean-field calculation of the actual ion [in a recent modification,<sup>25</sup> the energy  $\Delta_{\text{eff}}(m, n; m', n')$  was used instead]. Third, the configuration dependence of  $A(m, n)$  is neglected, and a common  $\bar{A}$  is calculated by assuming that a MF calculation for a *fixed* configuration  $e^{m_t n}$  incorporates in it the average multiplet effects of *all* configurations  $\{e^{m+n_t^0}, e^{m+n-1_t^1}, \dots, e^{0_t^m+n}\}$ . In the limit  $\lambda_e = \lambda_t = 1$ , this assumption gives<sup>23</sup>  $\bar{A} = (14B_0 - 7C_0)/9$ . Notice that while a MF calculation for  $e^{m_t n}$  indeed includes some average multiplet effect, it does so only for the single configuration energies that correspond to the configuration  $e^{m_t n}$  being considered and not others. Using this expression for  $\bar{A}$  and the free-ion integrals  $B_0$ , and  $C_0$ , this model expresses the multiplet energies in terms of  $\tilde{\lambda}_e$ ,  $\tilde{\lambda}_t$ , and  $\Delta_{\text{CF}}$ .

While it has been appreciated previously that the configuration dependence of  $A(m, n)$  greatly affects the multiplet spectra,<sup>47-49,52</sup> and that  $\Delta_{\text{CF}}$  is not interpretable in terms of MF energies,<sup>54</sup> it was not recognized that the problem can be simply transformed to a form where the explicit calculation of  $A(m, n)$  becomes unnecessary and, at the same time, the disposable parameter  $\Delta_{\text{CF}}$  is replaced by a well-defined, mean-field energy  $\Delta_{\text{eff}}$  that implicitly contains  $A(m, n)$ . This will be demonstrated in the next section.

#### IV. EFFECTIVE CRYSTAL-FIELD APPROACH

The present approach is based on Slater's ansatz that a mean-field electronic-structure calculation for a fixed configuration  $e^{m_t n}$  includes in its total energy  $E_T$  the average effect of all single-configuration energies that originate from the configuration  $(m, n)$ . There is no place in mean-field calculations for configuration mixing [Eq. (21)], or for single-configuration energies that do not belong<sup>23</sup> to the configuration  $e^{m_t n}$ , for which a self-consistent MF solution is sought.

We define the single-configuration average energy  $\hat{E}(m, n)$  as the weighted average of all  $E_{\text{SC}}^{(i)}(m, n)$  for multiplets  $i$  that evolve from the configuration  $e^{m_t n}$ , i.e.,

$$\hat{E}(m, n) = \sum_i \omega_i E_{\text{SC}}^{(i)}(m, n), \quad (28)$$

where the weights are taken over spin ( $S$ ) and space ( $g_\Gamma$ ) degeneracies:

$$\omega_i = (2S+1)g_\Gamma / \sum_{S, \Gamma} (2S+1)g_\Gamma. \quad (29)$$

Interestingly,  $\hat{E}(m, n)$  has the same universal form for all  $d^N$  arrangements, i.e.,

$$\hat{E}(m, n) = f_{m, n}(\lambda_e, \lambda_t) A(m, n) + g_{m, n}(\lambda_e, \lambda_t) (2B - C), \quad (30)$$

where  $f_{m, n}(\lambda_e, \lambda_t)$  and  $g_{m, n}(\lambda_e, \lambda_t)$  are fixed coefficients given in the Appendix. If we were to ignore differential hybridization<sup>48</sup> ( $\lambda = \lambda_e = \lambda_t$ ), we would have

$$f_{m, n}(\lambda) = [N(N-1)/2] \lambda^4$$

and all  $A$ 's would appear identically in all diagonal elements of  $d^N$ , as is the case in Racah's limit and in the Tanabe-Sugano-Kamimura approximation.  $g_{m, n}(\lambda)$ , however, is not a constant even in this limit.

We can now express the single-configuration energy  $E_{\text{SC}}^\alpha(m, n)$  of Eq. (17) relative to the average  $\hat{E}(m, n)$  defining thereby the single-configuration shift  $\Delta E_{\text{SC}}^\alpha(m, n)$ :

$$\Gamma D_{\alpha\alpha}(m, n) = \hat{E}(m, n) + \Delta E_{\text{SC}}^\alpha(m, n) + k_{\alpha\alpha} \Delta_{\text{CF}}. \quad (31)$$

The usefulness of this partitioning lies in the fact that all dependence on the symmetric contribution  $A(m, n)$  is absorbed into  $\hat{E}(m, n)$  of Eq. (30), and the single-configuration shift  $\Delta E_{\text{SC}}^\alpha(m, n)$  depends only on  $\lambda_e$ ,  $\lambda_t$ ,  $B_0$ , and  $C_0$ , much like the off-diagonal elements of Eq. (21). Referring the average single-configuration energies  $\hat{E}(m, n)$  to some standard configuration  $\hat{E}(m^0, n^0)$ ,

$$\hat{E}(m, n) \equiv \hat{E}(m^0, n^0) + \Delta(m, n; m^0, n^0),$$

the diagonal element of the interaction matrix is

$$\begin{aligned} \Gamma D_{\alpha\alpha}(m, n) - \hat{E}(m^0, n^0) &= \Delta E_{\text{SC}}^\alpha(m, n) \\ &+ [\Delta(m, n; m^0, n^0) + k_{\alpha\alpha} \Delta_{\text{CF}}], \end{aligned} \quad (32)$$

where  $\hat{E}(m^0, n^0)$  is common to all diagonal elements and hence does not affect the multiplet splitting. The term in square brackets in Eq. (32) is denoted as the "effective crystal-field splitting"  $\Delta_{\text{eff}}(m, n; m^0, n^0)$  and represents the average energy separation between the configurations  $(m, n)$  and  $(m^0, n^0)$ , including both bare-ion ( $\mathcal{H}_0$ ) and mean-field ( $\langle \mathcal{H}_1 \rangle$ ) effects. It equals, therefore, the mean-field energy difference of Eq. (3), i.e., the total energy that separates the configurations  $(m, n)$  and  $(m^0, n^0)$ . The diagonal and nondiagonal elements are given, therefore, as

$$\Gamma D_{\alpha\alpha}(m, n) = \Delta E_{\text{SC}}^\alpha(m, n) + \Delta_{\text{eff}}(m, n; m^0, n^0), \quad (33)$$

$$\Gamma D_{\alpha\beta} = E_{\text{CM}}^{\alpha, \beta}(m, n; m', n'),$$

respectively, and depend on  $B_0$ ,  $C_0$ ,  $\lambda_e$ , and  $\lambda_t$  alone. The solution to the multiplet problem provides, therefore, the multiplet correction  $\Delta E^{(i)}(m, n)$  to the MF total energy relative to the reference configuration  $(m^0, n^0)$ .

If we choose the  $e^2$  configuration as reference, the complete matrix for our illustrative  $^3T_1$  case is

$$\begin{pmatrix} -\lambda_t^4(3B_0 - C_0) + [\Delta(0,2;2,0) + 2\Delta_{CF}] & -6\lambda_e\lambda_t^3B_0 \\ -6\lambda_e\lambda_t^3B_0 & \lambda_e^2\lambda_t^2(5B_0 - \frac{1}{2}C_0) + [\Delta(1,1;2,0) + \Delta_{CF}] \end{pmatrix}. \quad (34)$$

The diagonalization of this matrix will yield results that differ both from the Tanabe-Sugano-Kamimura results derived from Eq. (24),

$$\begin{pmatrix} -5B + 2\Delta_{CF} & -6B \\ -6B & 4B + \Delta_{CF} \end{pmatrix}, \quad (35)$$

and from results of the Hemstreet-Dimmock approach,

$$\begin{pmatrix} \frac{1}{9}\tilde{\lambda}_t^4(31B_0 - 7C_0) + 2\Delta_{CF} & -6\tilde{\lambda}_e\tilde{\lambda}_t^3B_0 \\ -6\tilde{\lambda}_e\tilde{\lambda}_t^3B_0 & \frac{1}{9}\tilde{\lambda}_e^2\tilde{\lambda}_t^2(50B_0 - 7C_0) + \Delta_{CF} \end{pmatrix}. \quad (36)$$

The striking difference is that in the Tanabe-Sugano-Kamimura formalism the separation between these multiplets does not depend on  $C$  at all, while in the present formalism it always has a contribution from  $C_0$ .

The central point here is that our transformation identifies both bare-ion ( $\Delta_{CF}$ ) and average multiplet effects ( $\Delta$ ) in the effective crystal-field splitting  $\Delta_{eff}$  of Eq. (32), and that the configuration dependence in  $A(m,n)$  is renormalized in  $\Delta$  in a way that permits direct comparison with electronic-structure calculations.

The three central quantities in our approach— $\lambda_e$ ,  $\lambda_t$ , and  $\Delta_{eff}$ —can be computed from electronic-structure calculations directly from their definitions. Together with

the free-ion values of  $B_0$  and  $C_0$  (Ref. 47), these can be used to obtain the multiplet structure. Alternatively, it is possible to reverse the process and determine  $\lambda_e$ ,  $\lambda_t$ , and  $\Delta_{eff}$  from experiment by fitting the spectra. In the following section we discuss the results of the latter approach, in which we analyze the spectra of  $3d$  impurities in ZnO, ZnS, ZnSe, and GaP, for which sufficient data exist, as well as for bulk oxides. In view of the availability of only a small number of observed transitions per ion (cf. Table I), we have used a single, average  $\Delta_{eff}$  parameter so that the theory has only three independent quantities:  $\Delta_{eff}$ ,  $\lambda_e$ , and  $\lambda_t$ . We have not attempted to obtain the best possible fit for any given system (presumably, this is possible if one were to use a few different  $\Delta_{eff}$  parameters and the

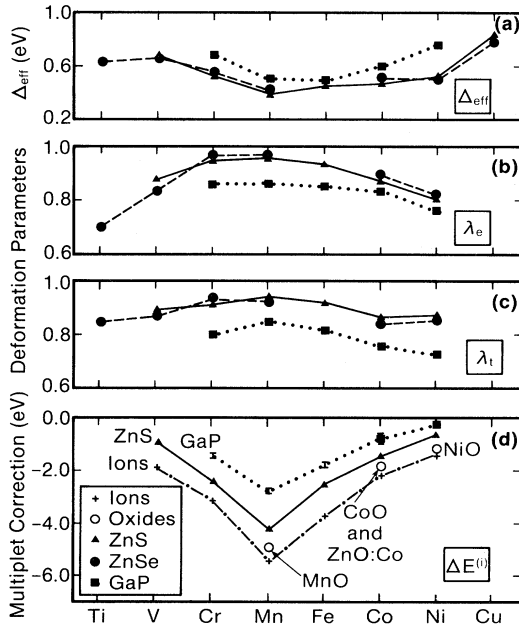


FIG. 2. Mean-field parameters obtained by fitting the  $d \rightarrow d^*$  absorption spectra of  $3d$  impurities in heteropolar semiconductors (Table I). (a) The effective crystal-field separation  $\Delta_{eff}$ , (b)  $e$ -orbital deformation parameter  $\lambda_e$ , (c)  $t_2$ -orbital deformation parameter  $\lambda_t$ , and (d) multiplet corrections to the ground-state energy for free ions, bulk oxides, and  $3d$  impurities in semiconductors.

TABLE III. Mean-field parameters deduced from the absorption spectra of divalent impurities in ZnS, ZnSe, and GaP. A range is given when less than three transitions are available.

System	$\lambda_e$	$\lambda_t$	$\Delta_{eff}$ (eV)
ZnO:Co	0.897	0.914	0.329
ZnS:V	0.876	0.897	0.670
ZnS:Cr	0.950	0.923	0.540
ZnS:Mn	0.967	0.938	0.402
ZnS:Fe	0.930	0.913	0.430
ZnS:Co	0.883	0.852	0.453
ZnS:Ni	0.806	0.870	0.520
ZnSe:V	0.830	0.870	0.666
ZnSe:Cr	0.975	0.940	0.540
ZnSe:Mn	0.970	0.926	0.40
ZnSe:Fe	0.93±0.04	0.91±0.04	0.41±0.03
ZnSe:Co	0.890	0.849	0.459
ZnSe:Ni	0.800	0.854	0.510
GaP:Cr	0.863±0.08	0.790±0.08	0.64±0.03
GaP:Mn	0.860±0.08	0.858±0.08	0.52±0.03
GaP:Fe	0.843±0.08	0.828±0.08	0.45±0.03
GaP:Co	0.831	0.759	0.608
GaP:Ni <sup>a</sup>	0.748	0.714	0.789
GaP:Ni <sup>b</sup>	0.814±0.0004	0.800±0.003	0.69±0.01

<sup>a</sup>Using data of Ref. 18.

<sup>b</sup>Using data of Ref. 15(b).

spin-orbit parameters), but we have instead aimed at achieving a good global fit for many systems, so that regularities can be identified.

## V. CHEMICAL TRENDS IN THE MEAN FIELD

### A. Trends in $\lambda_e$ , $\lambda_t$ , and $\Delta_{\text{eff}}$

Before describing some of the details of the optical spectra of  $3d$  impurities in heteropolar semiconductors (Sec. VI), we shall discuss the overall trends in the mean-field parameters  $\lambda_e$ ,  $\lambda_t$ , and  $\Delta_{\text{eff}}$  (Figs. 2(a)–2(c) and Table III). All results are assumed to pertain to substitutional impurities taking up the cation site, as has been the traditional assumption in this field.<sup>1–20</sup> In cases in which the number of observed transitions is smaller than the number of parameters in the model (cf. Table I), we provide the range of parameters (Table III) consistent with the data. All transitions occur in the  $2+$  oxidation state of the impurity: In II–VI semiconductors this corresponds to the neutral impurity  $A^0$ , whereas in III–V semiconductors the  $2+$  oxidation state corresponds to the negatively charged impurity  $A^-$ . Accordingly, we use the free-ion values<sup>47</sup> of  $B_0$  and  $C_0$  that correspond to the  $2+$  oxidation state.

Figure 2(a) displays a simple chemical regularity in the effective crystal-field splitting  $\Delta_{\text{eff}}$ : a minimum at Mn and a maximum at the high- $Z$  end of the series. A similar general trend was obtained in recent electronic-structure calculations for Si,<sup>25–28</sup> GaAs,<sup>21–23</sup> and GaP.<sup>26</sup> Interestingly, the existence of a minimum  $\Delta_{\text{CF}}$  at Mn was also observed in tetrahedrally coordinated  $3d$  complexes in solution<sup>20</sup> in comparing the series  $[(C_6H_5)_3AsO]_2NiCl_2$ ,  $(CoCl_4)^{2-}$ , and  $Cs_2MnCl_4$ , yielding  $\Delta_{\text{CF}}=0.52, 0.4,$  and  $0.25$  eV, respectively. The simple trend of  $\Delta_{\text{eff}}$  exhibited in Fig. 2(a) is in contrast with the complex  $S$ -shaped trend obtained previously with  $B$ ,  $C$ , and  $\Delta_{\text{CF}}$  fits,<sup>12</sup> a trend that is unmatched by any calculation. The ordering of  $\Delta_{\text{eff}}$  in an elemental sequence (often referred to as the “spectrochemical series”) shows an increase in  $\Delta_{\text{eff}}$  with increasing covalency  $C$  ( $C_{\text{GaP}} > C_{\text{ZnSe}} > C_{\text{ZnS}}$ ), as expected from simple chemical considerations.<sup>20</sup> It conflicts, however, with the expectation from the point-ion crystal-field theory<sup>20,51</sup> that predicts a scaling of the splitting  $10Dq$  with the fourth moment  $\langle 3d | r^4 | 3d \rangle$  of the bare-ion  $3d$  orbital (hence, a monotonic decrease with atomic number) and a rapid ( $l^{-5}$ ) decrease of  $10Dq$  with the impurity-ligand bond distance  $l$  [hence,  $\Delta(\text{ZnO}) > \Delta(\text{ZnS})$ ].

The trends in the orbital deformation parameters  $\lambda_e$  and  $\lambda_t$  in Figs. 2(b) and 2(c) (often<sup>20</sup> referred to as the “nephelauxetic series”) are likewise very simple: a maximum at Mn (except ZnSe:Cr, which is slightly higher than ZnSe:Mn) and a decrease with an increasing covalency of the host crystal (i.e., increased hybridization). In all cases, except for V and Ni in ZnS, and ZnSe, we find  $\lambda_e > \lambda_t$ , suggesting a stronger hybridization of the  $t_2$  orbitals (which form in tetrahedral-coordination  $\sigma$  bonds with the nearest-neighbor ligands) relative to the  $e$  orbitals (which form  $\sigma$  bonds only with the next-nearest ligands and weaker  $\pi$  bonds with the nearest neighbors). The same trend is evident in electronic-structure studies of  $3d$  impurities in Si,<sup>25,27</sup> GaAs,<sup>21,22</sup> and GaP.<sup>26</sup> We note that the orbital deformation parameters obtained here [cf. the definition in Eqs. (23) and (26)] are substantially larger

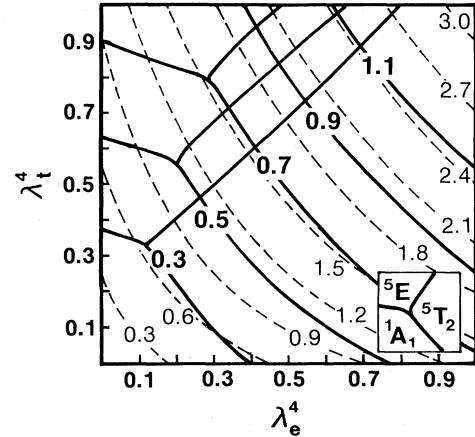


FIG. 3. Dependence of the multiplet correction (in eV) to the  ${}^5T_2$  state of the  $\text{Cr}^{2+}$  impurity ( $d^4$ ) on the  $e$ - and  $t_2$ -orbital deformation parameters  $\lambda_e$  and  $\lambda_t$  (dashed lines). The solid lines map the ground state of the system for a range of  $\Delta_{\text{eff}}$  values (in eV).

than those approximated by the  $d$ -orbital charge enclosed in a sphere<sup>21,23,25,28</sup> [charge localization of Eq. (27)], suggesting that the interelectronic repulsion in an impurity is closer to that of a free-ion than the charge localization is.

In the past<sup>20,48,51</sup> much emphasis has been placed on the decisive role of  $d$  orbitals, as opposed to  $p$ - $d$  hybridization, on the spectra of  $3d$  ions in complexes and in solids. The present calculation highlights the importance of the small but highly significant hybridization with ligand orbitals. We find that the energy of the multiplets is extremely sensitive to small reductions of  $\lambda_e$  and  $\lambda_t$  from unity. Hence, even a small radial expansion of the  $e$  orbital, or a  $p$ - $d$  hybridization in the  $t_2$  orbital, sensitively controls the spectra of the system. This is illustrated in Fig. 3, where we plot the multiplet correction for the  $\text{Cr}^{2+}(d^4)$  impurity in a  $T_d$  site. The dashed lines correspond to the value of the multiplet correction (in eV) associated with the  ${}^5T_2$  state of  $e^2t^2$  (the correction does not depend on  $\Delta_{\text{eff}}$ ). The solid lines map the symmetry of the ground states for different  $\lambda_e$ ,  $\lambda_t$ , and  $\Delta_{\text{eff}}$  for a range of  $\Delta_{\text{eff}}$ . Each of these phase diagrams is labeled by the appropriate value of  $\Delta_{\text{eff}}$ , also in eV. We see that for small values of  $\Delta_{\text{eff}}$  ( $\approx 0.3$ – $0.5$  eV), if  $\lambda_e$  deviates from unity by as little as 5%, the ground state switches from  ${}^5T_2(e^2t^2)$  to  ${}^5E(e^1t^3)$ , notwithstanding the large multiplet correction (2.7 eV) affecting the  ${}^5T_2$  state. Moreover, for large values of  $\Delta_{\text{eff}}$  and moderate hybridization ( $\lambda_e, \lambda_t \approx 0.8$ ), the low-spin multiplet  ${}^1A_1(e^4)$  becomes the ground state. As we approach the itinerant limit (small  $\lambda_e$  and  $\lambda_t$ ), multiplet corrections decrease rapidly and mean-field theory becomes an adequate representation.

### B. Trends in ground-state multiplet corrections

Figure 2(d) depicts the multiplet correction  $\Delta E^{(i)}(m, n)$  [Eq. (12)] to the ground state of the  $3d$  impurities. It also includes results for the bulk Mott insulators NiO, CoO, and MnO, as well as for free  $3d$  ions in their  $2+$  oxidation state obtained by fitting their spectra. While these corrections are extremely small on the scale of the total-energy scale  $E_T$ , in all cases they are sufficient to stabilize

the high-spin (Hund's-rule) ground state (the multiplet notation is given later in Figs. 12–14). Chemical trends are again very transparent. First, the largest multiplet stabilization occurs for Mn with its highest spin ( $S = \frac{5}{2}$ ), and it decreases monotonically (but not symmetrically) as we go to either side of Mn in the  $3d$  series. Second, the multiplet correction decreases rapidly with covalency in going from the free ions to oxides, sulfides, and phosphides (presumably, for Si:TA, for which no absorption spectra have yet been recorded, the corrections are still smaller). Introduction of a  $3d$  impurity into a covalent crystal results, therefore, in a larger loss of multiplet-stabilization energy relative to an impurity in a more ionic system. This will be discussed further in Sec. VII. Third, the correction for the impurity system ZnO:Co is virtually identical to that obtained for bulk CoO, suggesting that much of the multiplet effect is confined to the nearest-neighbor ligand cage. Fourth, the octahedrally coordinated bulk Mott insulators NiO, CoO, and MnO fit the general trend observed for dilute impurities.

Since the spectra of  $\text{Co}^{2+}$  were observed in a number of host crystals, this provides an opportunity to inspect the chemical trends in  $\lambda_e$ ,  $\lambda_t$ , and  $\Delta_{\text{eff}}$  with the host crystal. Figure 4 depicts this information (solid circles) for ZnO, ZnS, ZnSe, and GaP. It is evident that  $\Delta_{\text{eff}}$  is very small in a highly ionic system such as ZnO (0.340 eV, although it has the smallest lattice parameter); is similar in ZnS (0.453 eV) and ZnSe (0.459 eV), which have nearly identical anion electronegativities, and increases in going to the covalent GaP (0.61 eV). The deformation parameter  $\lambda_e$  varies slowly with the covalency of the host crystal, whereas the deformation parameter  $\lambda_t$  discriminates one

host crystal from the other. This is understandable<sup>63</sup> in light of the fact that the  $d$  part ( $l=2$ ) of the  $e$  orbital can mix only with a  $g$  orbital ( $l=4$ ) in tetrahedral symmetry. On the other hand, the  $d$  part of a  $t_2$  orbital can mix in tetrahedral symmetry already with  $p$  states; hence,  $\lambda_t$  varies from one host crystal to the other, reflecting the position of the atomic  $d$  state relative to the host  $t_2$  density of states. We notice that the trends obtained with the method of O'Neill and Allen<sup>49</sup> (open circles in Fig. 4), showing  $\Delta_{\text{eff}}(\text{ZnSe}) < \Delta_{\text{eff}}(\text{ZnS})$  and  $\lambda_e(\text{ZnO}) < \lambda_e(\text{ZnS})$ , appear at odds with the simpler chemical trends obtained here. In a similar analysis within the  $B$ ,  $C$ , and  $\Delta_{\text{CF}}$  theory, Hennel<sup>64</sup> studied the dependence of the Racah parameter  $B$  on the electronegativity of the host anion. He concluded that  $B$  is nearer its free-ion value  $B_0$  when the electronegativity of the host's anion increases, in agreement with the trends obtained here for the deformation parameters. Our analysis suggests further that the values of  $B$  for  $\text{Co}^{2+}$  in ZnS and ZnSe would be very similar.

## VI. OPTICAL TRANSITIONS IN $3d$ IMPURITIES

In this section we analyze in some detail the optical transitions of  $3d$  impurities, comparing the present assignments with those suggested previously. Figures 5 and 6 display the multiplet structure obtained in the present work, together with the observed transitions for TA impurities in ZnS and ZnSe, respectively. For the latter, we used the labels given in the experimental work. We used, wherever possible, energies for the maximum of the absorption band as opposed to zero-phonon energies. The experimental energies denoted by asterisks were used to obtain our fits to  $\lambda_e$ ,  $\lambda_t$ , and  $\Delta_{\text{eff}}$ . The others are predicted.

### A. $\text{Ni}^{2+}$ in ZnS and ZnSe

The ground state of the substitutional neutral  $\text{Ni}^{2+}$  ion is supposed to be  ${}^3T_1(F)$ , originating predominantly from the configuration  $e^4t^4$ . We associated the three main lines detected experimentally with the spin-allowed transitions  ${}^3T_1(F) \rightarrow {}^3T_2$ ,  ${}^3T_1(P)$ , and  ${}^3A_2$ . The experimental data were obtained from the work of Roussos and Schulz<sup>8</sup> for ZnS, and of Wray and Allen<sup>9</sup> for ZnSe. Our overall analysis matches the analysis of Roussos and Schulz carried out within the  $B$ ,  $C$ , and  $\Delta_{\text{CF}}$  theory in the assignment of the  $\beta$  band to the transitions to the ( ${}^1T_2, {}^1E$ ) states, the band  $\delta$  to the  ${}^1T_2$  state, the band  $\zeta$  to the  ${}^1T_1$  state (except that here the state  ${}^1A_1$  also contributes, contrary to the  $B$ ,  $C$ , and  $\Delta_{\text{CF}}$  results), and, lastly, the band  $\eta$  to the  ${}^1E$  state. It is worth noting that our results differ from the experimental spectrum for the  $\eta$  band, whereas the remaining transitions are in good agreement. The analysis of the ZnSe: $\text{Ni}^{2+}$  spectra is similar to that of ZnS: $\text{Ni}^{2+}$ . We note, however, that contrary to the  $B$ ,  $C$ , and  $\Delta_{\text{CF}}$  analysis, we predict the excited  ${}^3A_2$  state to be below the  ${}^1T_2$  state.

### B. $\text{Co}^{2+}$ in ZnS and ZnSe

The ground state for substitutional neutral  $\text{Co}^{2+}(d^7)$  is supposed to be  ${}^4A_2$ , originating from the configuration  $e^4t^3$ . We performed a fit to the absorption spectra associating the three observed lines with the transitions  ${}^4A_2 \rightarrow {}^4T_2$ ,  ${}^4T_1(F)$ , and  ${}^4T_1(P)$ . The experimental data

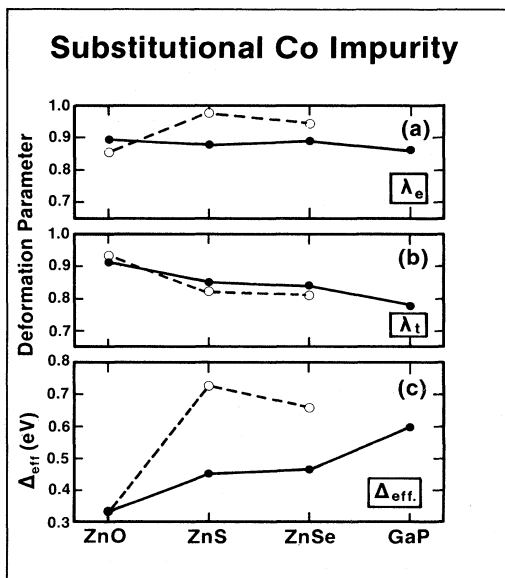


FIG. 4. Variations in the effective crystal-field energy  $\Delta_{\text{eff}}$  and  $e$ - and  $t_2$ -orbital deformation parameters  $\lambda_e$  and  $\lambda_t$  with the host crystal for the substitutional  $\text{Co}^{2+}$  impurity in various semiconductors. Solid circles indicate the results of the present study; open circles are results obtained with the O'Neill and Allen method (Ref. 48). All crystals except ZnO (the wurzite structure) have a cubic zinc-blende structure.



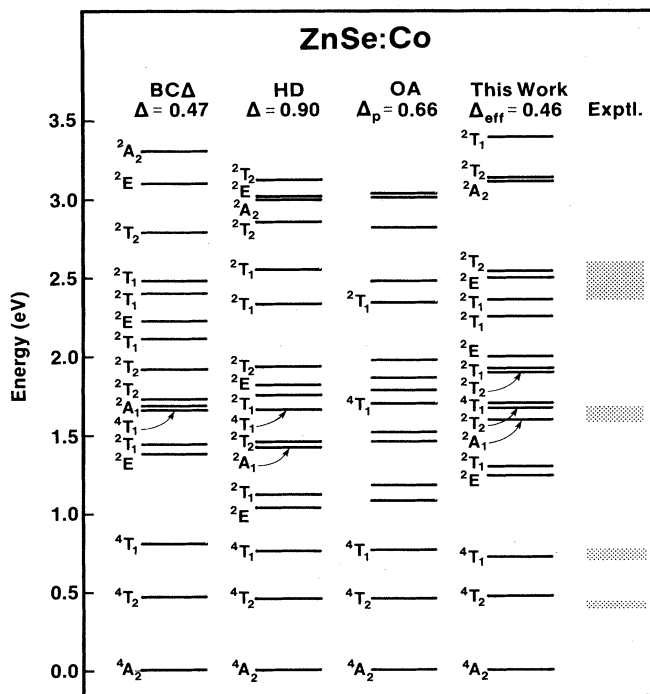


FIG. 7. Comparison of the multiplet structure of  $\text{ZnSe:Co}^{2+}$  as obtained by fitting the same data (Ref. 12) with four different multiplet methods: the Hemstreet-Dimmock (HD) approach (Ref. 23), the O'Neill-Allen (OA) method (Ref. 49), the Tanabe-Sugano  $B, C$ , and  $\Delta_{CF}$  method (Ref. 48), and the present method. Note the differences in the crystal-field energies  $\Delta$  obtained by the various methods.

these three lines with intra- $d$  excitations. In the case of  $\text{ZnS:Co}^{2+}$  only two lines were detected at 2.545 and 2.72 eV, again in agreement with our results; however, the two doublets we obtain lie very close to each other compared with the absorption data.

The results for  $\text{ZnSe:Co}^{2+}$  obtained by fitting the same experimental data with four different multiplet approaches are compared in Fig. 7. The spectra obtained by the Hemstreet-Dimmock (HD) and the O'Neill-Allen (OA) methods are almost identical, although they correspond to widely different crystal-field parameters. Notice that we find an excitation gap, argued by O'Neill and Allen to be essential to an explanation of the absence of non-radiative decay in this system.<sup>49</sup>

### C. $\text{Fe}^{2+}$ in ZnS

It is known from optical measurements<sup>65-67</sup> that the ground state of the  $\text{Fe}^{2+}$  impurity in ZnS is  $^5E$ , the absorption energy for the transition to the first excited state  $^5T_2$  being around 0.422 eV (3400  $\text{cm}^{-1}$ ). In a recent work, Skowronski and Liro<sup>6(a)</sup> performed a detailed study of the spin-forbidden transitions in this system. In their analysis of the absorption lines (see Fig. 5) they associated the line labeled  $P$  (16707  $\text{cm}^{-1}$ , or 2.071 eV) with the transition  $^5E \rightarrow ^3A_2$ , and the line labeled  $R$  (17217  $\text{cm}^{-1}$ , or 2.134 eV) with the  $^5E \rightarrow ^3A_1$  transition. In Fig. 5 we present the spectrum obtained by the present method, fitting the same three transitions used by Skowronski and

Liro.<sup>6(a)</sup> We interpret the  $M$  band as being formed by the transition to the state  $^3T_1$ , although there is a discrepancy ( $\sim 0.08$  eV) with the experimental results. The transitions to the states  $^3T_1$ ,  $^3T_2$ , and  $^3E$  form the  $N$  band, and the  $S$  band is composed of transitions to the states  $^3T_1$ ,  $^3T_2$ , and  $^1E$  (in the  $B, C$ , and  $\Delta_{CF}$  analysis the  $^1E$  state is not included in this band). Interestingly, the  $S$  band around 2.2–2.3 eV was shown<sup>6(a)</sup> to have an asymmetric form, suggesting that it overlaps with the donor photoionization (Fano resonance). This suggests that  $E(0/+)$  is around 2.1 eV (cf. footnote e to Table II).

### D. $\text{Mn}^{2+}$ in ZnS and ZnSe

The neutral  $\text{Mn}^{2+}$  impurity in II-VI semiconductors has the  $^6A_1$  ground state. This case ( $d^5$ ) is unique in that all transitions are spin forbidden. We based our study on the optical-absorption data of Gumlich *et al.*<sup>5</sup> for  $\text{ZnS:Mn}^{2+}$ , and the data collected by Wray and Allen<sup>9</sup> for  $\text{ZnSe:Mn}^{2+}$ . We present in Fig. 5 our theoretical spectrum along with the results of Gumlich *et al.* For this case, the significant differences between the  $B, C$ , and  $\Delta_{CF}$  approach and the present one are manifested in the relative position of the  $^4E$  and  $^4A_1$  levels. In the  $B, C$ , and  $\Delta_{CF}$  approach those states are always degenerate for any value of the parameters; in our treatment, they split due to the covalency effects included via the deformation parameters  $\lambda_e$  and  $\lambda_t$ .

In a recent work, Blanchard and Parrot<sup>68</sup> studied the covalency effect on the pair  $^4E(G), ^4A_1$  by inserting a multiplicative factor  $\tau$  in the Coulomb integrals involving the impurity  $t_2$  orbital for the states  $^6A_1, ^4E$ , and  $^4A_1$ . In this way,  $\tau^2$  is a measure of  $t_2$  covalency, whereas the  $e$  impurity orbital is still considered to be a pure- $d$  state. For a value of  $\tau^2 \simeq 0.92$ , they found a splitting  $^4E-^4A_1$  of about 1000  $\text{cm}^{-1}$ . As shown in Fig. 2 and Table III, we obtain values of  $\lambda_t = 0.938$  and  $\lambda_e = 0.967$ , which shows that for  $\text{Mn}^{2+}$  in ZnS there also exists a finite covalency of the  $e$  orbitals, so that we obtain for the splitting a value of 390  $\text{cm}^{-1}$ . In Fig. 8 we plot the dependence of the splitting of the two levels on the parameter  $\lambda_t^4$ , maintaining  $\lambda_e^4 = 1$ . The results show that the transition to the state  $^4A_1$  is always energetically higher than that to the  $^4E$  state. Two other absorption lines (around 2.77 and 3.22 eV) were observed experimentally, which we associate with transitions to the states  $^2T_2$ , and  $^4T_1$ .

### E. $\text{Cr}^{2+}$ in ZnS and ZnSe

The chromium impurity in II-VI compounds is found in the high-spin configuration  $e^2t^2$ , with ground state  $^5T_2$ . The symmetry around the impurity is lowered, however, to  $D_{2d}$  by a static Jahn-Teller effect,<sup>69</sup> and it is well established<sup>69</sup> that the spin-allowed transition  $^5B_2(^5T_2) \rightarrow ^5A_1(^5E)$  occurs around 5525  $\text{cm}^{-1}$  in ZnSe. The experimental data used here are obtained from the work of Grebe, Roussos, and Schulz<sup>10</sup> for  $\text{ZnSe:Cr}^{2+}$ , and that of Grebe and Schulz<sup>4</sup> for  $\text{ZnS:Cr}^{2+}$ . We will discuss the first system in more detail.

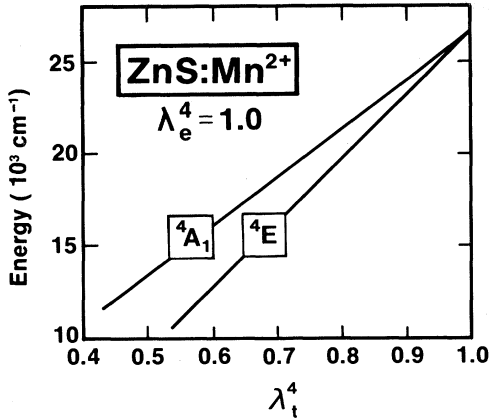


FIG. 8. Dependence of the multiplet correction to the  ${}^4A_1$  and  ${}^4E$  states of  $\text{ZnS:Mn}^{2+}$  on the  $t_2$ -orbital deformation parameter.

For  $\text{ZnSe:Cr}^{2+}$ , Grebe, Roussos, and Schulz<sup>10</sup> detect transitions at 2.033, 1.854, 1.606, 1.426, and 1.110 eV (16 400, 14 950, 12 950, 11 500, and 8950  $\text{cm}^{-1}$ , respectively). The authors analyze the spectrum within the  $B$ ,  $C$ , and  $\Delta_{\text{CF}}$  approximation, which fails to describe the transition at around 8950  $\text{cm}^{-1}$ , that is, it is not possible to obtain a good fit of the other transitions and simultaneously obtain a band at this energy, for both compounds. In a first interpretation, the authors associated the excitation in the region  $\sim 10\,000\text{ cm}^{-1}$  in  $\text{ZnS}$  with the  ${}^5T_2 \rightarrow {}^1A_1$  transition but if they leave out this strongly spin-forbidden transition, they obtain a better fit to the remaining lines.

An analysis of the experimental spectra shows that the intensity of the transitions is higher for the higher-energy region. Thus, we based our fitting procedure for  $\text{ZnSe:Cr}^{2+}$  on the value for the spin-allowed  ${}^5T_2 \rightarrow {}^5E$  transition (5525  $\text{cm}^{-1}$ ), searching at the same time for lines at 12 950 and 14 950  $\text{cm}^{-1}$ . Our results (Figs. 5 and 6) can be summarized as follows: The line at 16 400  $\text{cm}^{-1}$  is associated with a transition to the state  ${}^3E$ , the line at 14 590  $\text{cm}^{-1}$  with one to  ${}^3T_1$ , and the line at 12 950  $\text{cm}^{-1}$  with one to  ${}^3T_2$ . We find, at lower energies, a  ${}^3T_1$  state that we relate to the line at 11 500  $\text{cm}^{-1}$ , and the  ${}^1A_1$  state also appears at 9680  $\text{cm}^{-1}$  and can be related according to our results to the line at 8950  $\text{cm}^{-1}$ . The relative position of this  ${}^1A_1$  level is an interesting case for a comparison of the  $B$ ,  $C$ , and  $\Delta_{\text{CF}}$  and the present methods because it is the only state produced by the configuration  $e^4$  [hence  $\Delta E_{\text{SC}}=0$  in Eq. (17)], and it comes from the lowest-energy configuration (hence  $\Delta_{\text{eff}}=0$ ). Thus, its energy can be affected only by configuration mixing with the other  ${}^1A_1$  states, and this is a relatively small effect. The state  ${}^5T_2$  has no configuration mixing, but its energy is affected both by  $\Delta_{\text{eff}}$  and  $\lambda_e, \lambda_t$  (through  $\Delta E_{\text{SC}}$ ). In Fig. 9 we show a comparison of the energy diagrams for the states  ${}^1A_1$ ,  ${}^5E$ , and  ${}^5T_2$  obtained by the two models. First, for the  $B$ ,  $C$ , and  $\Delta_{\text{CF}}$  diagram, for which we used the values from Ref. 10, we have separated, for clarity, the contribution from  $\hat{E}(m,n)$ . Second, we show the results of the present approach. The extreme left and right columns thus corre-

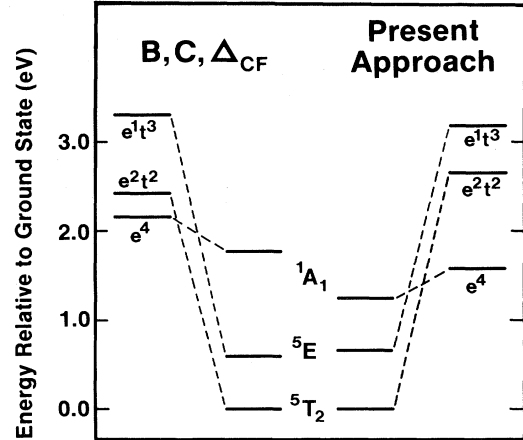


FIG. 9. Comparison of the multiplet structure for the  ${}^1A_1$ ,  ${}^5E$ , and  ${}^5T_2$  states of the  $\text{Cr}^{2+}$  impurity using the  $B$ , and  $C$ ,  $\Delta_{\text{CF}}$  approach and the present method. We set the ground state of  ${}^5T_2$  at the same energy for comparison.

spond to the average total energies ( $B$ ,  $C$ , and  $\Delta_{\text{CF}}$  method and the present method, respectively) of each configuration, and the center columns correspond to the energies of the multiplet states, already including configuration mixing. What is apparent from the figure is that the energy separation between the configurations  $e^4$  and  $e^2t^2$  is strikingly different; this is a consequence of the way the two-electron interactions are treated in the two models, namely that the contribution of the symmetric part of the interactions [the  $A(m,n)$  energies] to the multiplet splitting is ignored in the  $B$ ,  $C$ , and  $\Delta_{\text{CF}}$  method, so that the greater stability of the  $e^4$  configuration in the solid has to be accounted for only by the one-electron parameter  $\Delta_{\text{CF}}$  coupled to a reduction of the parameter  $2B - C$  that determines the initial separation of configuration energies. There are bounds to the variation of these parameters, set by the other transition energies, so that it is not feasible to bring the  ${}^1A_1$  state down in the  $B$ ,  $C$ , and  $\Delta_{\text{CF}}$  approach. In this particular case, the explicit dependence on differential hybridization in our approach is not the main factor affecting the  ${}^1A_1$ - ${}^5T_2$  splitting. Instead, the main contribution comes from the configuration dependence of the Racah parameter  $A$ , that is,  $A(e^4)$  differs considerably from  $A(e^2t^2)$ .

#### F. $\text{V}^{2+}$ in $\text{ZnS}$ and $\text{ZnSe}$

The oxidation state of the vanadium impurity in II-VI and III-V semiconductors is still the subject of serious controversy,<sup>3,70</sup> particularly concerning the assignment of the observed intra- $d$  optical transitions to  $\text{V}^{3+}$ ,  $\text{V}^{2+}$ , or  $\text{V}^+$ . Here we have assumed that the oxidation state  $\text{V}^{2+}$  pertains to the experimental spectra of  $\text{ZnS:V}$  and  $\text{ZnSe:V}$  observed by Hoang and Baranowski,<sup>3</sup> following these authors. For the fitting procedure, we assumed  ${}^4T_1$  symmetry for the ground state.

The symmetry assignments for the observed lines are very similar for both compounds, and an interesting

feature is the position of the  ${}^2E$  state originating mainly from the  $e^3$  configuration. In both cases, this  ${}^2E$  state appears close to the ground state (0.1 eV above the  ${}^4T_1$  state for ZnSe and 0.21 eV for ZnS), indicating that the impurity system is already near the low-spin regime. These results disagree with previous  $B$ ,  $C$ , and  $\Delta_{CF}$  analyses of ZnSe:V $^{2+}$ , which assign the  ${}^2E$  state to the broad absorption band around 0.78 eV (we interpret this band as being formed by two states,  ${}^2T_1$  and  ${}^2T_2$ ). We suggest that in more covalent materials such as III-V compounds e.g., GaP), where we would have smaller  $\lambda_e$  and  $\lambda_t$ , and a larger  $\Delta_{eff}$ , the V $^{2+}$  impurity will probably present a low-spin ( ${}^2E$ ) ground state.

### G. Absorption spectra of transition-atom impurities in GaP

In Table I we present the experimental data for the  $d \rightarrow d^*$  optical transitions used in this work for substitutional TA impurities in GaP. Notice that only for the impurities Co and Ni are there three observed lines for the 2+ oxidation state. For the remaining ions, Fe, Mn, and Cr, only one transition was observed. We give, therefore, the ranges of the mean-field parameters (Table III) consistent with the data. For the 3+ oxidation state (neutral impurity), only a single  $d \rightarrow d^*$  transition has been observed for V $^{3+}$  (Ref. 71).

Our fitting procedure for Ni and Co is similar to that of the II-VI host crystals; assuming the ground-state symmetry  ${}^4A_2$  for Co $^{2+}$  and  ${}^3T_1$  for Ni $^{2+}$ , we search for the set  $\lambda_e$ ,  $\lambda_t$ , and  $\Delta_{eff}$  that provides the best fit for the observed lines, subject to the constraint that the transitions involve high-spin states.

Our results for Co $^{2+}$  are consistent with the analysis of Baranowski *et al.*<sup>12</sup> and Weber *et al.*,<sup>72</sup> where the broad band around 0.89–1.03 eV (1.4–1.2  $\mu\text{m}$ ) is assigned to the transitions  ${}^4A_2 \rightarrow [{}^4T_1(F), {}^2E, {}^2T_1]$ . The situation with GaP:Ni is more complex. If we assume, following Baranowski *et al.*,<sup>18</sup> that the three observed transitions for GaP:Ni at 0.705, 1.24, and 1.426 eV correspond to excitations of the negatively charged impurity (i.e., Ni $^{2+}$ ,  $d^8$ ), we obtain a good fit with  $\lambda_e = 0.748$  eV,  $\lambda_t = 0.714$  eV, and  $\Delta_{eff} = 0.789$  eV. This fit identifies the three transitions as  ${}^3T_1(F) \rightarrow {}^3T_2$ ,  ${}^3T_1(P)$ , and  ${}^3A_2$ , respectively. Recently, Kaufmann *et al.*<sup>15(b)</sup> suggested that the lowest transition at 0.705 eV is related to the doubly negative impurity (i.e., Ni $^{1+}$ ,  $d^9$ ), and that the correct first excited state of the negative impurity is located at 0.583 eV [zero-phonon line (ZPL)] rather than at 0.705 eV. We examine this suggestion by attempting to fit the three excitation energies, 0.583, 1.24, and 1.426 eV, in the Ni $^{2+}$  model. The best fit indicates that the order of transition is different:  ${}^3T_1(F) \rightarrow {}^3T_2$ ,  ${}^3A_2$ , and  ${}^3T_1(P)$ . Nevertheless, the center of the first transition occurs at energies equal or larger than 0.65 eV (i.e., the maximum would be at 0.07 eV above the ZPL) in the investigated range of  $\Delta_{eff}$ . This best fit corresponds to the parameter set  $\lambda_e = (0.814 \pm 0.004)$ ;  $\lambda_t = (0.800 \pm 0.003)$ , and  $\Delta_{eff} = (0.69 \pm 0.01)$  eV.

In the cases of Fe and Cr, we assume that the observed lines correspond to a transition between the high-spin states  ${}^5E$  and  ${}^5T_2$ , and ground-state symmetries  ${}^5E$  for Fe $^{2+}$  and  ${}^5T_2$  Cr $^{2+}$ . We find Cr $^{2+}$  to be already close to

the low-spin regime (Fig. 3). For the Mn $^{2+}$  impurity we assumed the ground state to be  ${}^6A_1$ . For a reasonable range of  $\lambda_e$ ,  $\lambda_t$ , and  $\Delta_{eff}$ , the line at 1.34 eV is associated with the transition  ${}^6A_1 \rightarrow {}^4T_1$ . Recent<sup>26</sup> MF calculations for 3d impurities in GaP show good agreement with the mean-field portions of the experimental data as analyzed here.

### H. The Mott insulator CoO

The same procedure used to analyze the multiplet structure for 3d impurities can be extended to the stoichiometric limit of transition-metal compounds. Here, we discuss the case of the Mott insulator CoO; a more complete discussion of the series NiO, CoO, and MnO is deferred to a planned future publication. We use here the data of Pratt and Coelho.<sup>73</sup>

For the octahedrally coordinated CoO, the ground state is supposed<sup>74</sup> to be  ${}^4T_1$ , originating predominantly from the configuration  $e^4t^3$ . Table IV shows the results of applying the present method to the observed spectra of CoO, along with the traditional  $B$ ,  $C$ , and  $\Delta_{CF}$  assignment. Note that the  ${}^2E$  excited state appears near the  ${}^4T_2$  state in the band ranging from 0.9 to 1.033 eV, considerably lower than the  $B$ ,  $C$ , and  $\Delta_{CF}$  value. The value  $\Delta_{eff} = 0.743$  eV is considerably lower than that obtained by a  $B$ ,  $C$ , and  $\Delta_{CF}$  fit and removes the hitherto unexplained discrepancy with a high-quality molecular-orbital study<sup>74</sup> producing  $\Delta_{eff} = 0.691$  eV. The orbital deformation parameters  $\lambda_e^2 = 0.94$  and  $\lambda_t^2 = 0.70$  indicate that the  $t_2$  band is considerably more hybridized than the  $e$  band, which remains nearly atomic. A similar situation occurs for NiO, where a  $B$ ,  $C$ , and  $\Delta_{CF}$  fit yields a crystal-field splitting of 1.13 eV, markedly higher than the calculated value,<sup>74,75</sup> 0.724 eV, whereas the present approach produces in the fit  $\Delta_{eff} = 0.75$  eV, in excellent agreement with the results of electronic-structure calculations.<sup>74,75</sup>

## VII. CRYSTAL-FIELD STABILIZATION ENERGY

In this section we use the experimentally deduced crystal-field energies  $\Delta_{eff}$  [Fig. 2(a)] and ground-state mul-

TABLE IV. Observed and fitted absorption spectra of CoO. In parentheses we designate the final excited state obtained in the present calculation and in the  $B$ ,  $C$ , and  $\Delta_{CF}$  fit of Ref. 73. Our results correspond to  $B_0 = 0.1382$  eV,  $C_0 = 0.5413$  eV,  $\Delta_{eff} = 0.7430$  eV,  $\lambda_e^2 = 0.94$ , and  $\lambda_t^2 = 0.70$ . Experimental results from Ref. 73. Note the substantial differences in assignment of states in the present approach relative to a  $B$ ,  $C$ , and  $\Delta_{CF}$  fit.

Observed lines (eV)	Present fit	$B$ , $C$ , and $\Delta_{CF}$ fit
0.9–1.033	0.93 ( ${}^2E$ ) 1.11 ( ${}^4T_2$ )	1.033 ( ${}^4T_2$ )
1.610	1.570 ( ${}^2T_1$ )	1.212 ( ${}^2E$ )
2.026	2.008 ( ${}^4A_2$ )	1.927 ( ${}^2T_1$ )
2.053	2.080 ( ${}^2T_2$ )	2.054 ( ${}^2T_2$ )
2.137	2.231 ( ${}^2A_1$ )	2.201 ( ${}^4A_2$ )
2.26–2.33	2.31 ( ${}^4T_1$ )	2.300 ( ${}^4T_1$ )
2.50–2.56	2.43 ( ${}^2T_1$ )	2.659 ( ${}^2T_1$ )
2.605	2.601 ( ${}^2T_1$ )	2.803 ( ${}^2A_1$ )

triplet corrections  $\Delta E^{(i)}$  [Fig. 2(d)] to discuss the “open-shell contributions” to the cohesive energies of 3d coordination compounds. The binding energy of a guest atom to a host lattice is composed of closed-shell and open-shell cohesive interactions. In the absence of both multiplet effects and  $e-t_2$  crystal-field splitting (e.g., for compounds of closed-shell ions such  $\text{Ca}^{2+}$ ,  $\text{Zn}^{2+}$ ,  $\text{Sc}^{3+}$ , and  $\text{Ga}^{3+}$ ), the bonding is decided by closed-shell, one-electron effects such as covalent hybridization, increase in kinetic energy upon compression, orthogonality at ligand sites, electrostatic interactions with the other nuclei, and interelectronic repulsions. Experimental evidence suggests<sup>20</sup> that these sources of bonding  $E_b^0$  usually vary smoothly and monotonically with the position of the atom in the row of the Periodic Table. This evidence<sup>20</sup> consists of the observed smooth increase in the lattice energies of chalcogen and halide compounds of closed-shell ions with the cation’s atomic number, similar variations in the heat of ligation (e.g., with  $\text{H}_2\text{O}$ ), and in bond distances of such bare-ion coordination compounds. The smooth variations of  $E_b^0$  also underlie the concept of smooth variations in atomic or ionic radii of atoms having complete shells in their bonding state.<sup>76,77</sup> If, on the other hand, both crystal-field-splitting effects and multiplet corrections exist (e.g., guest ions with open 3d shells), the variations in cohesive properties are no longer smooth or monotonic (e.g., the cohesive energies of Ti, V, Cr, Fe, Ni, and Co chalcogenides and halides are substantially smaller than those expected from interpolating between the cohesive energies of closed-shell ions such as  $\text{Ca}^{2+}$  and  $\text{Zn}^{2+}$  chalcogenides and halides<sup>20</sup>). These deviations have been attributed to crystal-field-splitting effects,<sup>20,50,78,79</sup> i.e., the excess energy gained in the solid by occupying  $e$  and  $t_2$  levels whose baricenter lies below the free-ion 3d level. This energy is depicted by the dashed lines in Fig. 10 where we have used the experimentally deduced effective crystal-field splitting  $\Delta_{\text{eff}}$  for the various impurities (Table III). This crystal-field stabilization energy (CFSE)  $[(2n-3m)\Delta/5$  for  $e^m t^n$  configurations in tetrahedral fields,<sup>20</sup> or the negative of this quantity for octahedral fields] vanishes for  $\text{Mn}^{2+}$  (where the baricenter of the half-filled  $d^5$  shell in the  $e^2 t^3$  configuration coincides in the simple crystal-field model with the energy of the free-ion 3d level), and increases as one moves away from Mn to either side of the 3d series. These variations in the CFSE (except that less reliable values of  $\Delta_{\text{eff}}$  have been used) had been widely used<sup>20,50,78,79</sup> in the past to explain a large body of chemical data pertaining to excess stability of compounds with open-shell ions relative to compounds with closed-shell ions, or the relative stability of octahedral- versus tetrahedral-coordination compounds.<sup>20,79</sup> We wish to point out that this classical argument is at best incomplete as it leaves out the multiplet effects associated with open-shell atoms. These corrections have the opposite effect of the CFSE and offset its contribution.

The open-shell contribution to the cohesive energy consists both of a CFSE term and of a multiplet correction term  $\Delta E^{(i)}$  (solid)  $-\Delta E^{(i)}$ (atom) that reflects the loss in many-electron stabilization energy in going from the more localized free ion to the more extended states in the solid [compare the difference between the two multiplet correc-

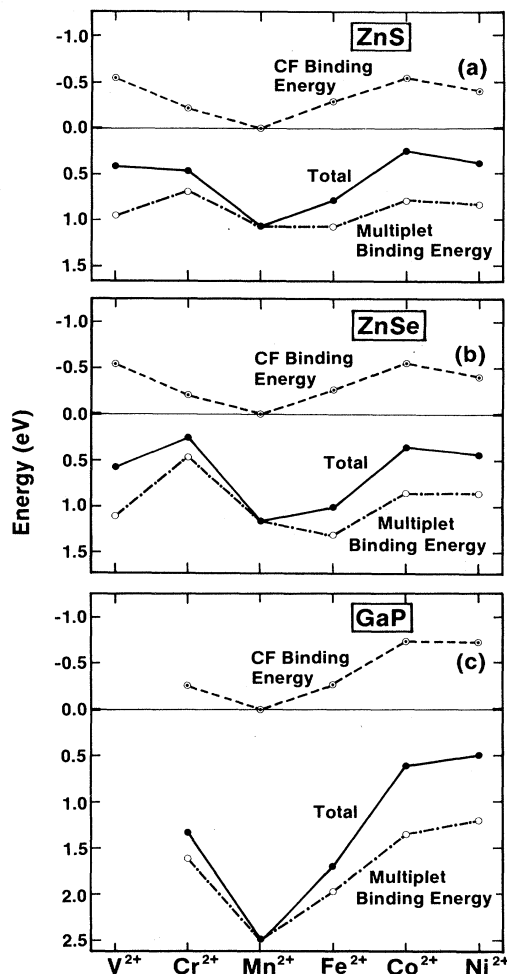


FIG. 10. Variations in the crystal-field stabilization energies (CFSE, dashed lines), multiplet contribution to the cohesive energy (dashed-dotted line), and their sum (total open-shell contribution to binding, solid line) for TA impurities in (a) ZnS, (b) ZnSe, and (c) GaP. Notice that the destabilizing multiplet correction to cohesive energy outweighs the CFSE.

tions in Fig. 2(d)]. The dotted-dashed lines in Fig. 10 depict this loss of multiplet energy in the solid relative to the free ion. This repulsive multiplet contribution to the cohesive energy is seen to be large for covalent host crystals such as GaP [e.g., 2.5 eV/atom for GaP:Mn; cf. Fig. 10(c)], since much of the multiplet stabilization is lost in the solid due to delocalization of the orbitals. It is substantially less repulsive in the more ionic host crystals such as ZnS [e.g., 1 eV/atom in ZnS:Mn; cf. Fig. 10(a)]. Hence, we predict from this analysis that the solubility of a 3d ion would increase rapidly as the covalency of the host crystal is reduced in going from Si to III-V and II-VI semiconductors. Few observations are in line. We note that the multiplet destabilization is larger than the crystal-field stabilization, so that sum of the two contributions (solid line in Fig. 10) is *positive*, having, hence, a net *destabilizing* effect. Open-shell contributions are thus more properly termed “crystal-field *destabilization*” ef-

fects. The reason that Mn coordination compounds have anomalously small cohesive energies and anomalously large bond lengths lies, therefore, in their large *destabilizing* multiplet correction rather than their vanishing *stabilizing* CFSE. Since the multiplet correction in the solid relative to the free ion depends sensitively on *sp* hybridization of the *d* orbitals (covalency), it is this effect (not the pure *d*-electron effect underlying CFSE) that controls much of the stability of the system. This has been pointed out recently from a pseudopotential point of view.<sup>80–82</sup> We believe that the myth of the predominance of *d*-electron CFSE effects<sup>20,78,83,84</sup> is largely based on the remarkable (but superficial) resemblance of the trends in CFSE (dashed lines in Fig. 10) to the trends in the total open-shell contribution (solid lines in Fig. 10). The physical origin (and even the sign) of both effects is, however, quite different.

Using the concept of the open-shell contribution to the cohesive energy, we can further analyze the data for bulk oxides and compare different limits of crystal-field configurations. Figure 11 shows the total open-shell contribution to the cohesive energy of the Mott insulators MnO, CoO, and NiO (connected by a dotted line to guide the eye). For MnO, the vanishing CFSE and the large positive multiplet correction add up to produce a destabilizing term (0.55 eV) in the cohesive energy. In contrast, the larger (negative) CFSE and the smaller positive multiplet correction in CoO and NiO add up to produce a total *stabilizing* contribution to the cohesive energy (−0.30 and −0.74 eV, respectively). As we move to TA impurities in a less ionic host crystal (e.g., in ZnSe; Fig. 11), the impurity states become more delocalized relative to oxides, resulting in a larger loss of multiplet stabilization energy in going from free ions to the solid. The attractive CFSE is now outweighed by the repulsive multiplet energy, producing a net destabilizing effect. Bulk oxides (or impurities in ZnO) are thus unique in that open-shell effects *stabilize* these systems. In contrast, impurities in covalent semiconductors have a large destabilizing open-shell con-

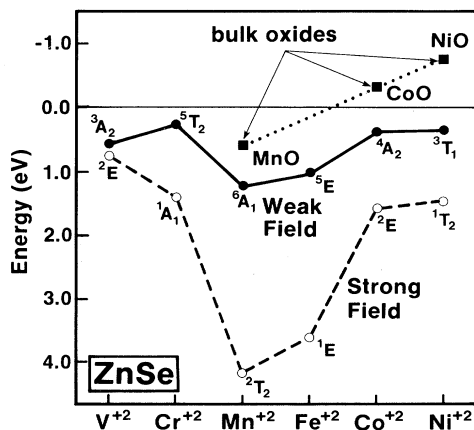


FIG. 11. Total open-shell contribution to the cohesive energy. Solid squares represent results for bulk oxides, whereas circles represent results for 3*d* impurities in ZnSe. Note that the weak-field (high-spin) configurations (solid line) are stabler than the strong-field (low-spin) configurations (dashed line).

tribution, resulting in an overall small substitutional solubility that, nevertheless, will increase as the host crystal becomes more ionic. This nonclassical effect can explain the trends in solubility, whereas the classical explanation based on the mismatch between the impurity and host atomic radii fails to do so (e.g., Zn and Ga have similar classical radii).

In Fig. 11 we compare the total open-shell contribution to the cohesive energy of TA impurities in ZnSe using the high-spin (weak-field) configuration (solid line) and the low-spin (strong-field) configuration (dashed line). Clearly, in the low-spin limit the destabilizing multiplet effect is much larger than in the high-spin configuration. If multiplet effects are ignored and only CFSE is used to compare the energies of the low- and high-spin configurations of *d*<sup>3</sup> through *d*<sup>6</sup>, the low-spin arrangement is predicted to be more stable, in contrast with experiment (e.g., Refs. 1 and 2).

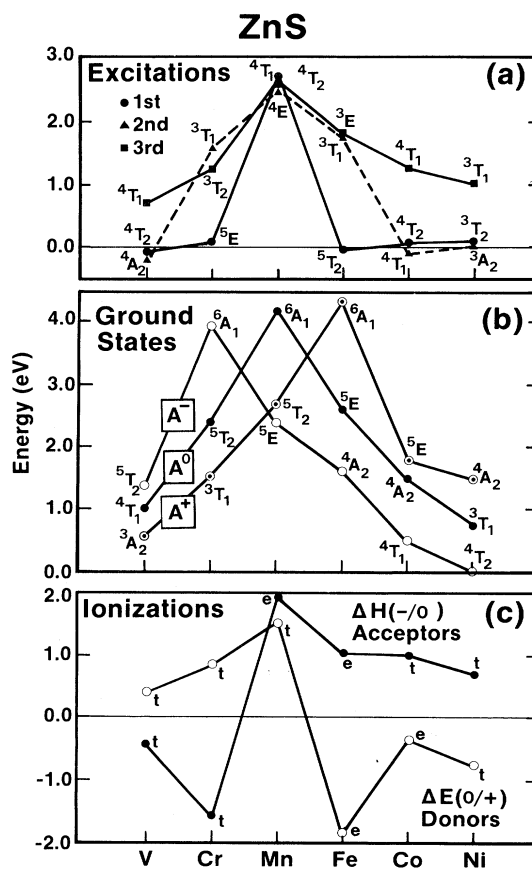


FIG. 12. Multiplet corrections for 3*d* impurities in ZnS. (a) Correction to the three lowest high-spin *d*→*d*\* excitation energies of the neutral (*A*<sup>0</sup>) impurity [cf. Eq. (13)]. The labels pertain to the multiplet of the final states. (b) Negative of the correction to the ground state of the neutral *A*<sup>0</sup> (i.e., TA impurity of charge state 2 + ), positively charged *A*<sup>+</sup> (i.e., TA impurity of charge state 3 + ), and negatively charged *A*<sup>-</sup> (i.e., TA impurity of charge state 1 + ) impurities [cf. Eq. (12)]. Only the results for *A*<sup>0</sup> are fitted to experiment. (c) Multiplet corrections for acceptor [ $\Delta H(-/0)$ , cf. Eq. (14)] and donor [ $\Delta E(0/+)$ , cf. Eq. (15)] ionizations. The labels *e* or *t* refer to the one-electron orbital being ionized.

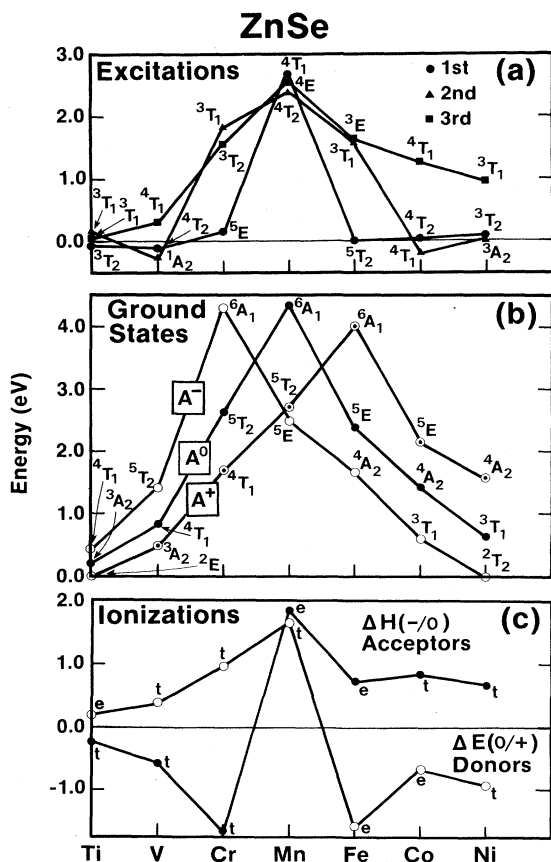


FIG. 13. Multiplet corrections for 3d impurities in ZnSe. See caption to Fig. 12.

### VIII. CHEMICAL TRENDS FOR EXCITATION AND IONIZATION ENERGIES

#### A. $d \rightarrow d^*$ excitation energies

Having obtained the mean-field parameters  $\lambda_e$ ,  $\lambda_t$ , and  $\Delta_{\text{eff}}$  from the absorption spectra, we are in a position to evaluate the multiplet correction

$$\Delta E^{(j)}(m', n') - \Delta E^{(i)}(m, n)$$

for excitation energies calculated in MF approaches [e.g., Eq. (30)] between states  $i$  and  $j$  [cf. Eq. (13)]. Figures 12(a), 13(a), and 14(a) display this correction for the three lowest excited states of TA impurities in ZnS, ZnSe, and GaP, respectively. The symmetries of the final states are indicated in each case. The symmetry of the initial ground state is given in Table I. We note the following salient features. First, the lowest excited state has a very small multiplet correction in all crystals for all impurities but Mn, for which the multiplet correction in the ground state ( ${}^6A_1$  with spin  $\frac{5}{2}$ ) far exceeds that in the excited state ( ${}^4T_1$  with spin  $\frac{3}{2}$ ) because of the decrease in total spin attendant upon excitation. Hence, mean-field theory may work well for the first excitation energy of all impurities except Mn as a result of an effective cancellation between the many-electron corrections in the ground and ex-

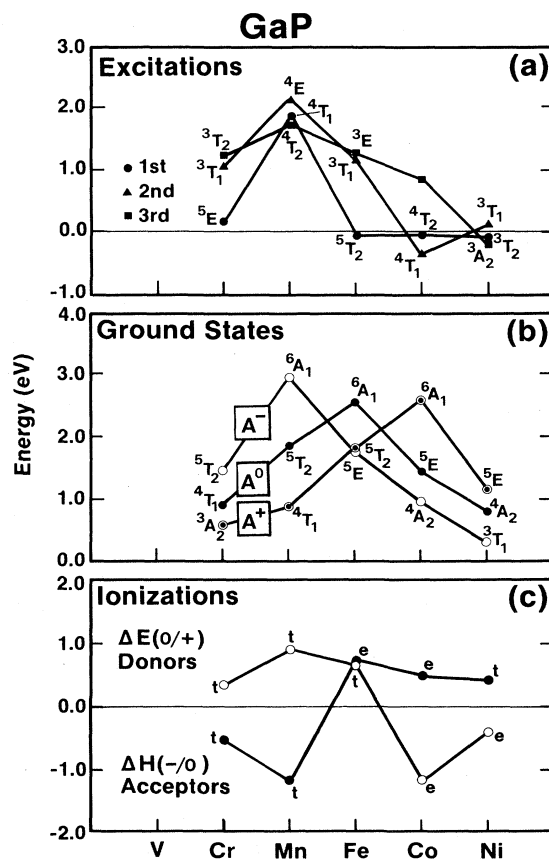


FIG. 14. Multiplet corrections for 3d impurities in GaP. (a) Corrections to the three lowest high-spin  $d \rightarrow d^*$  excitation energies of the negatively charged  $A^-$  impurity [cf. Eq. (13)]. The multiplet labels denote the final states. (b) Negative of the correction to the ground state  $A^0$  (i.e., TA impurity of charge state 3+), positively charged  $A^+$  (i.e., TA impurity of charge state 4+), and negatively charged  $A^-$  (i.e., TA impurity of charge state 2+) impurities [cf. Eq. (12)]. Only the results for  $A^-$  are fitted to experiment. (c) Multiplet corrections for acceptor [ $\Delta H(-/0)$ , cf. Eq. (14)] and donor [ $\Delta E(0/+)$ , cf. Eq. (14)] ionizations. The labels  $e$  or  $t$  refer to the one-electron orbital being ionized.

cited states.<sup>25</sup> Second, the multiplet corrections have a maximum at Mn for all three excited states, and they decrease monotonically on both sides of the 3d series. These corrections can be substantial even if the spin is conserved in the excitation process. Third, multiplet corrections for excitations can be both positive (increasing the energy relative to the MF results) and negative (producing a lower excitation energy relative to the MF results, e.g., the second excited state of Co). Fourth, there is no overall trend in the multiplet correction with the excitation energy; however, the corrections are reduced with the covalency of the host crystal. Nevertheless, the corrections for the second and third excited states are substantial on the physically relevant scale of the band gap (up to 80% of the gap even in GaP). We conclude that with the exception of the first excited state in all impurities but Mn, a correct mean-field electronic-structure calculation cannot

TABLE V. Multiplet correction energy for the ground and the three lowest excited states of divalent impurities in ZnS. Some of the multiplets involve a single one-electron configuration (e.g., ground state of Cr, Mn, Fe, and Co). Others involve configuration mixing. We list separately the contribution to the total multiplet energy from such interconfigurational interactions. This effect accounts for all of the multiplet corrections in some cases (e.g., second excited state of  $\text{Cr}^{2+}$ ).

Impurity	Multiplet	Predominant configuration	Total multiplet correction (eV)	Configuration-mixing energy (eV)	Multiplet	Predominant configuration	Total multiplet correction (eV)	Configuration-mixing energy (eV)
Ground state								
$\text{V}^{2+}$	${}^4T_1$	$e^2t^1$	-1.012	-0.101	${}^4T_2$	$e^1t^2$	-1.100	0.0
$\text{Cr}^{2+}$	${}^5T_2$	$e^2t^2$	-2.414	0.0	${}^1A_1$	$e^4$	-0.295	-0.295
$\text{Mn}^{2+}$	${}^6A_1$	$e^2t^3$	-4.43	0.0	${}^4T_2$	$t^3e^2$	-1.4901	-0.320
$\text{Fe}^{2+}$	${}^5E$	$e^3t^3$	-2.636	0.0	${}^3T_1$	$e^4t^2$	-0.827	-0.266
$\text{Co}^{2+}$	${}^4A_2$	$e^4t^3$	-1.511	0.0	${}^4T_1$	$e^2t^5$	-1.646	-0.295
$\text{Ni}^{2+}$	${}^3T_1$	$e^4t^4$	-0.701	-0.130	${}^3A_2$	$e^2t^6$	-0.640	0.0
First excited state								
$\text{V}^{2+}$	${}^2E$	$e^3$	-0.119	-0.119	${}^2T_2$	$e^2t^1$	-0.071	-0.359
$\text{Cr}^{2+}$	${}^5E$	$e^1t^3$	-2.330	-0.0	${}^3T_1$	$e^3t^1$	-0.763	-0.203
$\text{Mn}^{2+}$	${}^4T_1$	$e^3t^2$	-1.684	-0.170	${}^4E$	$e^2t^3$	-1.791	-0.219
$\text{Fe}^{2+}$	${}^5T_2$	$e^2t^4$	-2.410	0.0	${}^3E$	$e^3t^3$	-0.783	-0.307
$\text{Co}^{2+}$	${}^4T_2$	$e^3t^4$	-1.436	0.0	${}^2E$	$e^4t^3$	-0.202	-0.202
$\text{Ni}^{2+}$	${}^3T_2$	$e^3t^5$	-0.609	0.0	${}^1T_2$	$e^4t^4$	0.464	-0.108
Second excited state								
Third excited state								

legitimately reproduce the observed excitation energies of  $3d$  impurities.

Table V gives the multiplet corrections for the ground and first three excited states of the TA impurities in ZnS. We show separately the configuration-mixing contribution to the multiplet correction. In the ground state, the multiplet correction for all impurities but  $\text{V}^{2+}$  and  $\text{Ni}^{2+}$  arises purely from anisotropic interelectronic interactions within a single configuration, whereas for  $\text{V}^{2+}$  and  $\text{Ni}^{2+}$  the configuration mixing contributes only 10%. On the other hand, configuration mixing becomes progressively more dominant in the excited states; for the  ${}^1A_1$  excited state of  $\text{Cr}^{2+}$  and the  ${}^2E$  excited state of  $\text{Co}^{2+}$  configuration-mixing constitutes all of the multiplet correction. In cases where interconfigurational many-electron interactions dominate, one-electron theory is clearly inapplicable.

#### B. Donor and acceptor ionization energies

Since the observed excitation processes for  $3d$  impurities pertain to the  $A^0$  charge state in II-VI semiconductors and the  $A^-$  charge state in III-V semiconductors (in both cases the oxidation state of the impurity is  $2+$ ), the fit to the excitation spectra produces just the mean-field parameters for these states. In what follows we will estimate the chemical trends in the other charged state by assuming, for lack of better information,<sup>85</sup> that the orbital deformation parameters  $\lambda_e$  and  $\lambda_t$  that pertain to the  $2+$  oxidation state are approximately valid also for the oxidation states  $3+$  and  $1+$ . Notice that the multiplet correction does not depend on  $\Delta_{\text{eff}}$  in the absence of configuration mixing and has only a weak dependence on it otherwise. Using this procedure, we find that the ground-state symmetries agree with the assignments from EPR and optical techniques where available, i.e., in III-V semiconductors for  $\text{Fe}^{3+}$  (Ref. 40),  $\text{Ni}^{3+}$  (Ref. 86), and  $\text{Cr}^+$  and  $\text{Cr}^{4+}$

[Refs. 2, 15(c), and 87].

Figures 12(b), 13(b), and 14(b) depict the multiplet corrections to the ground states of  $A^0$ ,  $A^+$ , and  $A^-$  in ZnS, ZnSe, and GaP, respectively. In all cases the largest correction occurs for the highest spin state,  ${}^6A_1$ . Note that the ordering of the correction is interchanged in the low- $Z$  limit ( $A^- > A^0 > A^+$ ), relative to the high- $Z$  limit ( $A^+ > A^0 > A^-$ ). Exactly the same trend occurs in the calculated exchange splitting in free ions (Fig. 15), suggesting that much of the multiplet stabilization is due to spin correlations.

Using the multiplet corrections to the ground states of  $A^0$ ,  $A^+$ , and  $A^-$ , we can further calculate their differences; i.e., the multiplet correction  $\Delta H(-/0)$  for the  $A^0 \rightarrow A^-$  acceptor transitions [Eq. (14)] and the correction  $\Delta E(0/+)$  for the  $A^0 \rightarrow A^+$  donor transitions [Eq. (15)]. These corrections to the mean-field predictions for donor and acceptor activation energies are displayed in Figs. 12(c), 13(c), and 14(c). We have labeled each point by the symbol  $e$  or  $t$ , denoting the orbital being ionized in the transition. The corrections are seen to be substantial on the scale of the band gap. For the V and Cr acceptors, the correction is negative in II-VI and III-V materials [shifting the acceptor level obtained in MF calculations towards the maximum (VBM)]. The opposite is true for Ni, Co, and Fe having positive acceptor corrections. The largest corrections occur for the Mn states in II-VI semiconductors and the Mn acceptor in III-V semiconductors, reflecting the combination of large deformation parameters [Figs. 2(b) and 2(c)] and small effective crystal-field splitting [Fig. 2(a)].

By subtracting the multiplet corrections  $\Delta H(-/0)$  and  $\Delta E(0/+)$  [Figs. 12(c)–14(c)] from the observed acceptor and donor energies, respectively (Table II), we can obtain [cf. Eqs. (14) and (15)] the corresponding ionization energy expected from MF theory. By the transition-state ar-

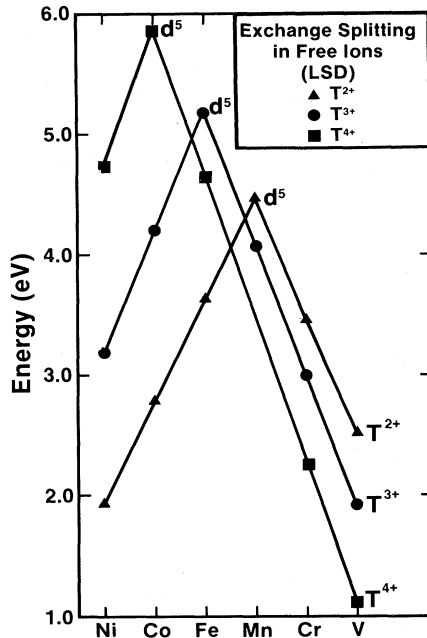


FIG. 15. Calculated exchange splitting (difference between spin-up and spin-down  $3d$  orbital energies) of  $3d$  ions in the local-spin-density approach. Note that the ordering and trends resemble those of the multiplet corrections to the ground states of  $A^0$ ,  $A^+$ , and  $A^-$  impurities [Figs. 12(b), 13(b), and 14(b)], suggesting that the latter are dominated by spin correlations.

gument surrounding Eqs. (8) and (9), this energy corresponds to the distance from the valence-band maximum (VBM) (for acceptors) or the conduction-band maximum (CBM) (for donors) of the transition-state  $e$  or  $t_2$  level from which the ionization occurs. Having obtained the  $e$  or  $t_2$  level position in this way, we can apply the experimentally deduced crystal-field energy  $\Delta_{\text{eff}}$  [Fig. 2(a)] and find the approximate position on the partner level. However, only the position of the levels deduced directly from experiment is reliable. Figure 16 displays the observed (thick horizontal lines) single-donor (in II-VI materials) and single-acceptor (in GaP) transition energies, along with the positions of the transition-state levels  $e$  and  $t_2$  deduced in this analysis. We indicate in each case the one-electron configurations which correspond to each transition in our analysis of the data. The partner levels (e.g.,  $e$  for Cr, Mn, and Ni in GaP) are included only to guide the eye. Since no donor levels are observed with certainty for ZnS:Mn and ZnSe:Mn, we predict these levels by the reverse process of extrapolating the transition-state  $t_2$  levels of the adjacent elements and applying the experimentally deduced multiplet correction  $\Delta E(0/+)$  of Figs. 10(c) and 11(c). We similarly predict the unobserved donor level in ZnSe:V using the ionization data for ZnSe:Ti (Ref. 34). The value of the donor level in ZnS:Ni is an estimate<sup>88</sup> (see subsection C following). The donor level in ZnS:Co is still controversial: compare Noras *et al.*,<sup>7</sup> in which it is suggested that the doublets at 2.3–2.6 eV in ZnS:Co and 2.5–2.7 eV in ZnS:Co are observed in absorption since they are degenerate with the

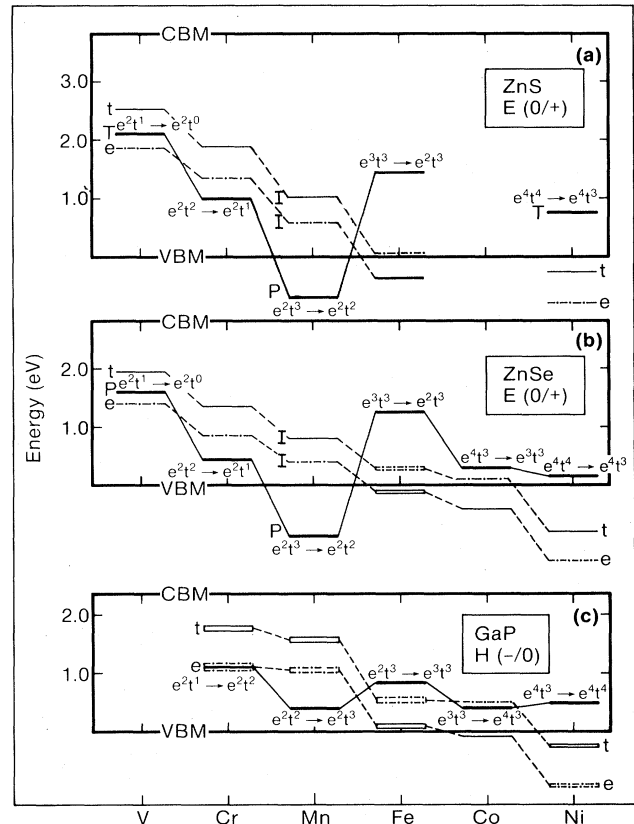


FIG. 16. Observed donor activation energies in ZnS and ZnSe [(a) and (b), respectively] and acceptor activation energies in GaP [part (c)], both denoted by thick horizontal solids lines. See Table II for references to the experimental work. The thin solid lines denote the positions of the transition-state one-electron levels deduced from the data. Note that the observed activation energies are nonmonotonic, whereas the deduced one-electron levels (from which the multiplet correction has been subtracted) are monotonic. The dominant one-electron configurations involved in the transitions [Eqs. (4)–(9)] are given, as predicted by the model. The partner level not involved in the transition is shown by the dashed-dotted line, only to guide the eye.  $T$  denotes tentative,  $I$  denotes interpolated, and  $P$  denotes predicted.

conduction bands, and hence borrow oscillator strength from them, with the recent interpretation in O'Neill and Allen<sup>49</sup> of the occurrence of a “gap” in the multiplet spectra, and the suggestion of Robbins<sup>44</sup> that the onset of the continuum in ZnSe:Co occurs at  $\sim 2.55$  eV. We hence omit this data (shown by us previously<sup>89</sup>) from Fig. 16. Similarly, the older value of  $E(0/+)$  for ZnS:Fe displayed by us before<sup>89</sup> has now been replaced by the more recent values [cf. Refs. 6(a) and (b) and Table II].

The trends observed in Fig. 16 are revealing. First, we see that the strong nonmonotonicity exhibited by the experimental donor and acceptor energies result from similar nonmonotonicities in the multiplet corrections  $\Delta H(-/0)$  and  $\Delta E(0/+)$ . Hence, mean-field theory should exhibit a simple monotonic trend of the  $e$  and  $t_2$  levels. This is indeed the hitherto unexplained trend observed in MF electronic-structure calculations for  $3d$  im-

TABLE VI. Calculated multiplet corrections (in eV) to the Coulomb repulsion energies for the neutral ( $A^0$ ) impurities. In parentheses we denote the one-electron levels  $e$  or  $t_2$  from which both donor and acceptor ionizations occur.

Host Oxidation state	ZnSe	ZnS	GaP
	2 +	2 +	3 +
Impurity			
Ni	-0.29 ( $t_2$ )	-0.31 ( $t_2$ )	
Co			-0.69 ( $e$ )
Fe	-0.88 ( $e$ )	-1.00 ( $e$ )	
Mn			-0.29 ( $t_2$ )
Cr	-0.72 ( $t_2$ )	-0.67 ( $t_2$ )	-0.19 ( $t_2$ )
V	-0.20 ( $t_2$ )	-0.22 ( $t_2$ )	

purities in GaAs,<sup>21,23</sup> GaP,<sup>26</sup> and ZnS.<sup>29</sup> The trend in the one-electron levels for a fixed impurity and changing host crystal is an increase in the binding energy as the ligand (anion) orbital becomes more tightly bound ( $E_{\text{ZnS}} > E_{\text{ZnSe}} > E_{\text{ZnTe}} > E_{\text{GaP}}$ ). This trend was explained previously.<sup>90</sup> Second, this analysis predicts that the donor state of ZnS:Mn and ZnSe:Mn will reside inside the VB, clarifying the fact that, despite persistent attempts, its determination still remains elusive.<sup>91</sup> Third, the analysis explains why Mn forms a shallow acceptor in III-V materials ( $E_{\text{VBM}} + 0.4$  eV in GaP and  $E_{\text{VBM}} + 0.14$  eV in GaAs) in terms of its large multiplet correction [Fig. 14(c)] associated with its large orbital deformation parameters [Figs. 2(b) and 2(c)]. Fourth, the theory predicts that the  $e$  level will disappear from the gap into the valence band in going from Fe to Co impurities in GaP and for the Fe impurity in ZnSe. It also predicts the position of the yet unobserved donor level in ZnSe:V.

### C. The Mott-Hubbard Coulomb energies

The present analysis makes it possible to calculate the multiplet correction to the mean-field approximation for the Coulomb repulsion energy  $U_{\text{MF}}$  [Eqs. (10) and (16)]. Table VI depicts the results for those systems that have a common one-electron level in both donor and acceptor transitions. It is seen that multiplet corrections tend to reduce Coulomb energies by substantial amounts, in particular at the center of the  $3d$  series. Hence, the stability of many charged states of transition-atom impurities in semiconductors results both from the reduction of  $U$  by nonlinear screening effects (the self-regulating response<sup>27,61</sup>) and from its reduction by many-electron multiplet effects. If  $\Delta U$  [Eq. (16)] is sufficiently negative, it could outweigh the relaxed  $U_{\text{MF}}$ , leading to the possibility of an “exchange-correlation negative effective  $U$ ” (likely to occur in GaAs:Mn).

Experimental data exists for the single-donor<sup>4,10,36</sup> and single-acceptor<sup>35,38,42,46</sup> transitions of Cr and Ni impurities in ZnS and ZnSe, as well as for the single-<sup>38,42</sup> and double-acceptor<sup>14,43</sup> transitions of Cr and Ni impurities in GaP (Table VII). Our analysis suggests that all of these transitions involve excitations of the one-electron  $t_2$  level. Hence, these data directly provide the experimental value of the  $t$ -orbital Mott-Hubbard energy  $U^{(tt)}$  for the  $2+$  ox-

idation state of Cr( $d^4$ ) and Ni( $d^8$ ) in three materials (sixth column in Table VII). Using the calculated multiplet correction  $\Delta U^{(tt)}$  for these transitions [Eq. (16) and seventh column in Table VII], we can further obtain the mean-field value  $U_{\text{MF}}^{(tt)}$  of the Mott-Hubbard energies (last column in Table VII). We see that multiplet effects reduce  $U^{(tt)}$  by sizable amounts and that these Coulomb energies in the more covalent host crystal GaP are about half of their values for the more ionic systems ZnS and ZnSe. For GaP:Fe, our analysis shows that the first- and second-acceptor transitions involve the ionization of the  $e$  orbitals rather than the  $t_2$  orbitals. A similar analysis hence reveals (last line in Table VII) a large Coulomb repulsion energy for the more localized  $e$  orbitals ( $U_{\text{MF}}^{(ee)} = 1.6$  eV). Notice also that the Coulomb repulsion energies could depend on the oxidation state of the impurity. For GaP:Cr we can use the first- ( $E_v + 1.12$  eV) and second- ( $E_v + 1.85$  eV) acceptor energies to find  $U^{(t)} = 1.85 - 1.12 = 0.73$  eV for the  $A^-$  center (i.e.,  $\text{Cr}^{2+}$ ). Using, however, the tentative value of  $E_v + (0.5 \pm 0.1)$  eV for the first donor of GaP:Cr (Ref. 15(c)) and the value  $E_v + 1.12$  eV for the first acceptor, we find  $U^{(ee)} = 1.12 - (0.5 \pm 0.1) = (0.62 \pm 0.1)$  eV for the  $A^0$  center (i.e.,  $\text{Cr}^{3+}$ ). Within the 0.1-eV experimental error, hence,  $U^{(ee)}(A^-) \cong U^{(ee)}(A^0)$ . Interestingly, this parallels theoretical observations<sup>26,27</sup> that one-electron binding energies are approximately linear with occupation numbers (hence their slope  $U$  is approximately constant).

Recall that, for free ions, the Coulomb energies for Cr and Ni are around 19–22 eV (Ref. 32 and Fig. 17 following), and that for  $3d$  impurities in silicon<sup>27</sup> the calculated values are as small as 0.2–0.3 eV. Since, however, Table VII shows that in heteropolar semiconductors  $U$  is quite large, Koopmans theorem (assuming  $U=0$ ) is clearly invalid. It is important to emphasize that the mean-field values of the Coulomb energies [Eq. (10)] correspond to total-energy differences for the appropriately relaxed lattice configurations. For example, the  ${}^5T_2(d^4)$  ground state of ZnSe:Cr is known to distort to a  $D_{2d}$  site symmetry through a Jahn-Teller (JT)  $E$  mode,<sup>69</sup> and that its first excited  ${}^5E$  state can, in principle, show a similar distortion. Further, the  ${}^5T_2 \rightarrow {}^6A_1$  excitations to the  $d^5$  ground state of the Cr impurity in II-VI semiconductors are accompanied by lattice distortions resulting in relaxation energies of about<sup>35</sup> 0.3–0.4 eV (compare optical and thermal values for the first-acceptor energies in Table VII). Kaminska *et al.*<sup>92</sup> obtain a small (about 0.04 eV) JT energy for Cr( $d^4$ ) in ZnS and ZnSe (see also Ref. 69). These relaxation energies were then ascribed to symmetry-conserving (i.e., breathing) modes by Godlewski and Kaminska.<sup>35</sup>

The role of relaxations for Ni in ZnS and ZnSe is not clear. In a recent work, Sokolov *et al.*<sup>36</sup> interpreted electroabsorption and cathode-luminescence results to suggest a donor transition of Ni( $d^8 \rightarrow d^7$ ) in ZnSe at  $E(0/+)=2.67$  eV. Intriguingly, however, Watts<sup>93</sup> reports the production of the Ni( $d^7$ ) EPR signal already at illumination with  $h\nu=2.07$  eV photons. For ZnS:Ni, Holton, Schneider, and Estle<sup>88</sup> report that the Ni( $d^7$ ) EPR signal could be produced by 3.1-eV photons, but the authors do not give the form of the photostimulation

TABLE VII. Experimental ionization energy levels for the neutral ( $A^0$ ) Cr and Ni impurities in ZnS, ZnSe, and GaP, given relative to the top of the valence band. The experimental Mott-Hubbard energies  $U^{MF}$  for the  $2+$  oxidation state ( $A^0$  in ZnS and ZnSe,  $A^-$  in GaP), the corresponding multiplet correction  $\Delta U$ , and the mean-field energies  $U_{MF}^{MF}$  are given in eV. Values marked with an asterisk correspond to equilibrium (i.e., relaxed) configurations. The notation  $t$  or  $e$  in the last column refers to the type of one-electron orbital involved in the ionization process.

Host	Impurity	Single donor	Single acceptor	Double acceptor	Hubbard energy $U^{MF}$ (expt.)	Multiplet correction $\Delta U^{MF}$ (calc.)	Mean-field $U_{MF}^{MF}$ (calc.)
ZnS	Cr	$E_v + 1.0^a$	$E_v + 2.78^b$		1.78		2.45 ( $t$ )
ZnS	Ni	$E_v + 0.75^c$	$E_v + 2.41^{b*}$ $E_v + 2.48^d$		1.41* 1.73	-0.67 -0.31	2.08* ( $t$ ) 2.04 ( $t$ )
ZnSe	Cr	$E_v + 0.46^c$	$E_v + 2.24^b$ $E_v + 1.93^{b*}$		1.78* 1.47*	-0.72	2.50* ( $t$ ) 2.49* ( $t$ )
ZnSe	Ni	$E_v + 0.15^f$	$E_v + 1.85^d$		1.70	-0.29	1.99 ( $t$ )
GaP	Cr		$E_v + 1.12^{g*}$	$E_v + 1.85^{h*}$	0.73*	-0.31	1.04* ( $t$ )
GaP	Ni		$E_v + 0.5^{i*}$	$E_v + 1.55^{j*}$	1.05*	0.18 <sup>k</sup> -0.24 <sup>l</sup>	1.23* ( $t$ ) 1.29 ( $t$ )
GaP	Fe		$E_v + 0.86^m$	$E_v + 2.2^n$	1.39	-0.21	1.60 ( $e$ )

<sup>a</sup>Reference 4.

<sup>b</sup>Reference 35.

<sup>c</sup>Reference 88, tentative (see text).

<sup>d</sup>Reference 46.

<sup>e</sup>Reference 10.

<sup>f</sup>Reference 36.

<sup>g</sup>Reference 38.

<sup>h</sup>Reference 43.

<sup>i</sup>Reference 42.

<sup>j</sup>Reference 14.

<sup>k</sup>Following interpretation of Ref. 18.

<sup>l</sup>Following interpretation of Ref. 15(b).

<sup>m</sup>Reference 40(a).

<sup>n</sup>Reference 45.

curve. Using the results of Sokolov *et al.*<sup>36</sup> for ZnSe:Ni, we obtain the Mott-Hubbard energy in Table VII. If we assume the  $U_{MF}^d$  of Ni( $d^8$ ) in ZnSe to be approximately valid also for ZnS (based on the overall similarity of the two systems), the onset of the donor transition in ZnS is predicted to occur at about  $h\nu = 3.05$  eV. This presents circumstantial evidence that the value of Holton, Schneider, and Estle can be taken as the donor energy of Ni( $d^8$ ) in ZnS, as indicated in Table VII and Fig. 16. We feel, however, that the appearance of the Ni( $d^7$ ) EPR signal in ZnSe (Ref. 93) at much lower photon energies than the donor energy,<sup>36</sup> as given by electroabsorption, deserves more experimental investigations, as it could indicate, among other effects, the occurrence of lattice relaxations.

### IX. ATOMIC ANALOG TO ACCEPTOR AND DONOR TRANSITIONS

In this section we illustrate the fact that the nonmonotonic trends in acceptor and donor energies have a simple atomic origin. Figure 17(a) depicts the observed single-acceptor energies [Table II and Ref. 43] of  $3d$  impurities in three different III-V semiconductors. In all cases, the acceptor energies have a local maximum at Fe and a local minimum at Mn, as discussed in the preceding section. The atomic analog of this phenomenon is illustrated in Fig. 17(b).

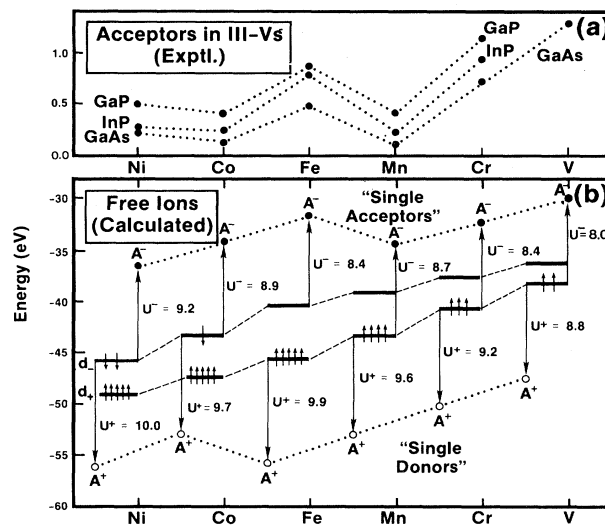


FIG. 17 (a) Experimental single-acceptor energies in III-V semiconductors, (b) calculated free-ion spin-polarized  $3d$  levels (horizontal thick solid lines), single-acceptor levels (solid circles), and single-donor levels (open circles). Note that the nonmonotonicity in the data (the Mn acceptor being at a lower energy than the Fe acceptor) is paralleled by the atomic acceptor levels but not by the atomic single-particle levels.

We first calculate the positions of the spin-up and spin-down  $3d$  orbital energies of free  $3d$  ions in their  $3+$  oxidation state (analogous to neutral substitutional impurities on the cation site in III-V semiconductors) using the local-spin-density formalism. These levels and their ground-state occupations are denoted by the thick horizontal lines in Fig. 17(b) and are seen to have a monotonically decreasing binding energy as one goes backwards in the  $3d$  series, much like the one-electron  $e$  and  $t_2$  levels for  $3d$  impurities in GaP [Fig. 16(c)]. Next, we calculate the change in the total energy  $U^+ \equiv E_T(A^+) - E_T(A^0)$  upon ionizing the  $3d$  ion and the change  $U^- \equiv E_T(A^-) - E_T(A^0)$  upon adding an electron to the same  $3d$  ion. In each case we ionize the electron from the highest occupied level and add an electron to the first available orbital. The vertical lines denoted  $U^+$  and  $U^-$  indicate the energy involved in each of these respective processes. Notice that  $U^+ + U^-$  is the atomic  $3d$  Coulomb energy  $U^{(dd)}$ , analogous to the impurity Coulomb energy in Eqs. (4) and (5), except that the extra electron or hole is placed inside the continuum bands in the latter case. In free ions, the Coulomb energies  $U^{(dd)}$ , are seen to range from 19.2 eV in  $\text{Ni}^{3+}$  to 16.8 eV in  $\text{V}^{3+}$ . Subtracting  $U^+$  from the orbital energy from which the electron is ionized produces the position of the ionic "single-donor" level (open circles), whereas adding  $U^-$  to the orbital energy to which an electron is added produces the "single-acceptor" level (solid circles). Free ions are obviously strongly "positive- $U$  systems" as the donor level lies well below the acceptor level.

Figure 17(b) shows that although the one-electron levels are monotonic functions of the impurity's atomic number, the ionic "single-acceptor" levels are not, showing a local maximum at Fe and a local minimum at Mn, much like the situation for the respective impurities [Fig. 17(a)]. The reason for this is obvious from Fig. 17(b): Whereas both donor and acceptor transitions in Ni and Co occur from the spin-down ( $d_-$ ) levels, the same transitions in Mn, Cr, and V occur from the spin-up ( $d_+$ ) levels, which are below the  $d_-$  levels. The separation between them (exchange splitting) leads to the nonmonotonic behavior. Two differences relative to the impurity case exist: (i) While the jump in energy between Mn and Fe is about 3 eV in the free ions, it is only about 0.5 eV for the impurities; (ii) the data<sup>1,43</sup> for the Co impurity show this acceptor level to be below that of Ni, whereas this nonmonotonicity has no counterpart in the free ions. We conclude that much of the multiplet corrections deduced experimentally for acceptor transitions in  $3d$  impurities [Figs. 12(b), 13(b), and 14(b)] are the result of spin correlation.

## X. SUMMARY

A new approach is proposed for the separation of many-electron multiplet effects and one-electron, mean-field effects in the spectra of  $3d$  impurities. Recently,<sup>94-96</sup> a number of attempts have been made to construct a theory of multiplets for atoms using local-density theory. It has become clear that, whereas one could construct single determinantal energies from linear combinations of multiplet energies, the reverse process of con-

structing multiplet energies from sums of single determinantal energies is nonunique. Fundamentally, the reason for this is that the exchange-correlation energy in local-density theory is taken to be symmetry independent. In the present work we avoid these problematics altogether by using a Hartree-Fock-type approach merely for separating the total energy into *average* multiplet effects and *distinct* multiplet effects. We then invoke Slater's ansatz that the total mean-field energy corresponds to an average over multiplet energies. We do not attempt to calculate the distinct multiplet energies from local-density theory, as attempted before.<sup>94-96</sup> Instead, we identify *differences* in mean-field total energies with the corresponding differences in average multiplet energies [Eqs. (3)-(11)] and correct these differences for *distinct* multiplet effects [Eqs. (12)-(16)] evaluated by analyzing the experimental data through a Hartree-Fock-type theory, not local-density theory. In the present method it is no longer necessary to identify a crystal-field parameter with a bare-ion energy,<sup>47,48</sup> nor to neglect the configuration dependence of the  $a_1$ -symmetric electron repulsion energy  $A$ .<sup>23,25</sup> The method is easier to apply than previous methods because of the simplicity of the interaction matrices (cf. the Appendix). It can be used either for predicting multiplet structure if the mean-field parameters  $\lambda_e$ ,  $\lambda_t$ , and  $\Delta_{\text{eff}}$  are available from calculations, or it can be used to fit experiment, thereby deducing the mean-field parameters. Analysis of the spectra of  $3d$  impurities in ZnO, ZnS, ZnSe, GaP, NiO, MnO, and CoO reveals the regular chemical trends of the mean-field parameters with the impurity and the host crystal. This analysis further permits the separation of many-electron multiplet effects from mean-field effects in excitation and ionization spectra. This separation reveals the chemical trends in the many-electron effects, showing their rapid reduction as the host crystal becomes less ionic. Using the experimentally deduced multiplet corrections, we can then find the excitation and ionization energies expected from an ideal mean-field calculation. This shows that many of the hitherto unexplained discrepancies between electronic-structure calculations and experiment are attributable to many-electron effects. Hence, the region where one-electron theory is expected to work is separated from the region where it is not; the corrections to the latter region are established from this analysis.

## ACKNOWLEDGMENTS

One of us (A.Z.) would like to thank the organizers of the fourth "Lund International Conference on Deep Level Impurities in Semiconductors," Eger, Hungary, May, 1983, where the author was exposed to many of the experimental observations that made this work possible. In particular, stimulating discussions with Paul J. Dean have instigated our interest in this problem. The authors thank B. Brandow, B. Clerjaud, U. Kaufmann, F. E. Williams, and J. W. Allen for directing us to many important references for experimental work. This work was supported in part by the Office of Energy Research, Material Science Division, U. S. Department of Energy, under Grant No.

TABLE VIII. Functions  $f_{m,n}(\lambda_e, \lambda_t)$  and  $g_{m,n}(\lambda_e, \lambda_t)$  that enter in the expressions for  $E(m, n)$ , for  $m+n=N$  and  $2 \leq N \leq 5$ .

$d^2$	$f$	$g$	$d^3$	$f$	$g$
$e^2$	$\lambda_e^4$	$-\frac{4}{3}\lambda_e^4$	$e^3$	$3\lambda_e^4$	$-4\lambda_e^4$
$et$	$\lambda_e^2\lambda_t^2$	$-\frac{1}{2}\lambda_e^2\lambda_t^2$	$e^2t^1$	$2\lambda_e^2\lambda_t^2 + \lambda_e^4$	$-(\lambda_e^2\lambda_t^2 + \frac{4}{3}\lambda_e^4)$
$t^2$	$\lambda_t^4$	$-\lambda_t^4$	$e^1t^2$	$\lambda_t^4 + 2\lambda_e^2\lambda_t^2$	$-(\lambda_t^4 + \lambda_e^2\lambda_t^2)$
			$t^3$	$3\lambda_t^4$	$-3\lambda_t^4$
$d^4$	$f$	$g$	$d^5$	$f$	$g$
$e^4$	$6\lambda_e^4$	$-8\lambda_e^4$	$e^4t^1$	$4\lambda_e^2\lambda_t^2 + 6\lambda_e^4$	$-(2\lambda_e^2\lambda_t^2 + 8\lambda_e^4)$
$e^3t^1$	$3\lambda_e^2\lambda_t^2 + 3\lambda_e^4$	$-(\frac{3}{2}\lambda_e^2\lambda_t^2 + 4\lambda_e^4)$	$e^3t^2$	$\lambda_t^4 + 6\lambda_e^2\lambda_t^2 + 3\lambda_e^4$	$-(\lambda_t^4 + 3\lambda_e^2\lambda_t^2 + \lambda_e^4)$
$e^2t^2$	$\lambda_t^4 + 4\lambda_e^2\lambda_t^2 + \lambda_e^4$	$-(\lambda_t^4 + 2\lambda_e^2\lambda_t^2 + \frac{4}{3}\lambda_e^4)$	$e^2t^3$	$3\lambda_t^4 + 6\lambda_e^2\lambda_t^2 + \lambda_e^4$	$-(3\lambda_t^4 + 3\lambda_e^2\lambda_t^2 + \frac{4}{3}\lambda_e^4)$
$e^1t^3$	$3\lambda_t^4 + 3\lambda_e^2\lambda_t^2$	$-(3\lambda_t^4 + \frac{3}{2}\lambda_e^2\lambda_t^2)$	$e^1t^4$	$6\lambda_t^4 + 4\lambda_e^2\lambda_t^2$	$-(6\lambda_t^4 + 2\lambda_e^2\lambda_t^2)$
$t^4$	$6\lambda_t^4$	$-6\lambda_t^4$	$t^5$	$10\lambda_t^4$	$-10\lambda_t^4$

DE-AC02-77-CH00178. Two of us (A.F.) and (M.J.C.) acknowledge support from the Fundação de Amparo à Pesquisa do Estado de São Paulo, Brasil.

#### APPENDIX

In this appendix we give the general form of the average configuration energies  $\hat{E}(m, n)$  for each configuration  $(m, n)$  of a  $d^N$  system, necessary for expressing the in-

teraction matrices of the two-electron Hamiltonian  $\hat{\mathcal{H}}_1$  in the form developed in this work.

The averages of multiplet energies for all terms within a particular configuration,  $\hat{E}(m, n)$ , are given in the form of Eq. (30) in Table VIII, for  $m+n=N$  from  $N=2$  up to  $N=5$ . For the complementary configurations  $d^6$ ,  $d^7$ , and  $d^8$  the corresponding average energies can be obtained by the relation

$$\begin{aligned} \hat{E}(4-m, 6-n) = & \hat{E}(m, n) + [5(3-n)\lambda_t^4 + 2(12-3m-2n)\lambda_e^2\lambda_t^2 + 3(2-m)\lambda_e^4]A \\ & + [5(n-3)\lambda_t^4 + (2n+3m-12)\lambda_e^2\lambda_t^2 + 4(m-2)\lambda_e^4](2B-C), \end{aligned} \quad (\text{A1})$$

where a configuration  $(m, n)$  corresponds to  $e^m t^n$ .

An important feature of this method is that the Hamiltonian matrices to be diagonalized do not change in going from  $d^N$  to  $d^{10-N}$ , since the diagonal elements do not include  $\hat{E}(m, n)$ . However, to reach the atomic limit in this method we need the values

$$\Delta(m, n; m', n') = \hat{E}(m, n) - \hat{E}(m', n').$$

The atomic limit can be defined as the situation  $\lambda_e = \lambda_t = 1$ ,  $A(m, n) \equiv A(d^N)$ , and  $\Delta_{CF} = 0$ . In this limit, it is easily seen that

$$\begin{aligned} \Delta_{\text{eff}}(m, n; m^0, n^0) = & \Delta(m, n; m^0, n^0) \\ = & [g_{m, n}(1, 1) - g_{m^0, n^0}(1, 1)](2B - C). \end{aligned} \quad (\text{A2})$$

As an example, for the  $d^4$  system in the atomic limit we have (choosing the  $e^4$  configuration as a reference)

$$\begin{aligned} \Delta_{\text{eff}}(4, 0; 4, 0) = & 0, \\ \Delta_{\text{eff}}(3, 1; 4, 0) = & \frac{5}{2}(2B - C), \\ \Delta_{\text{eff}}(2, 2; 4, 0) = & \frac{11}{3}(2B - C), \\ \Delta_{\text{eff}}(1, 3; 4, 0) = & \frac{7}{2}(2B - C), \\ \Delta_{\text{eff}}(0, 4; 4, 0) = & 2(2B - C). \end{aligned} \quad (\text{A3})$$

It is interesting to note that, as the quantity  $2B - C$  has a negative value, the  $e^4$  configuration (spin  $S=0$ ) has the higher energy in this limit, followed by the  $t^4$  configuration.

<sup>1</sup>Landolt-Börnstein Numerical Data and Functional Relationships in Science and Technology, edited by O. Madelung (Springer, Berlin, 1982), Vols. 17a and 17b.

<sup>2</sup>U. Kaufmann and J. Schneider, Adv. Electron. Electron Phys. **58**, 81 (1983).

<sup>3</sup>Le. M. Hoang and J. M. Baranowski, Phys. Status Solidi B **84**, 361 (1977).

<sup>4</sup>G. Grebe and H. J. Schultz, Phys. Status Solidi B **54**, K69 (1972).

<sup>5</sup>H. E. Gumlich, R. L. Pfrogner, J. C. Schaffer, and F. E. Williams, J. Chem. Phys. **44**, 3929 (1966).

<sup>6</sup>(a) M. Skowronski and Z. Liro, J. Phys. C **15**, 137 (1982); (b) F. F. Kodzhespirov, M. Bulanyi, and J. A. Tereb, Fiz. Tverd. Tela (Leningrad) **16**, 3159 (1974). [Sov. Phys.—Solid State **16**,

- 2052 (1975)].
- <sup>7</sup>J. M. Noras, H. R. Szawelska, and J. W. Allen, *J. Phys. C* **14**, 3255 (1981).
- <sup>8</sup>G. Roussos and H. J. Schultz, *Phys. Status Solidi B* **100**, 577 (1980).
- <sup>9</sup>E. M. Wray and J. W. Allen, *J. Phys. C* **4**, 512 (1971).
- <sup>10</sup>G. Grebe, G. Roussos, and H. J. Schulz, *J. Phys. C* **9**, 4511 (1976).
- <sup>11</sup>D. W. Langer and H. J. Richter, *Phys. Rev.* **146**, 554 (1966).
- <sup>12</sup>J. M. Baranowski, J. M. Allen, and G. L. Pearson, *Phys. Rev.* **160**, 627 (1967).
- <sup>13</sup>(a) K. P. O'Donnell, K. M. Lee, and G. D. Watkins, *J. Phys. C* **16**, 728 (1983); (b) J. H. Haanstra, in *II-VI Semiconducting Compounds*, edited by D. G. Thomas (Benjamin, New York, 1967), p. 207.
- <sup>14</sup>S. G. Bishop, P. J. Dean, P. Porteous, and D. J. Robbins, *J. Phys. C* **13**, 1331 (1980).
- <sup>15</sup>(a) U. Kaufmann, M. Ennen, and J. Weber, unpublished results quoted in Ref. 1, p. 218; (b) U. Kaufmann, W. H. Koschel, J. Schneider, and J. Weber, *Phys. Rev B* **19**, 3343 (1979); (c) U. Kaufmann and J. Schneider, *Appl. Phys. Lett.* **36**, 748 (1980).
- <sup>16</sup>A. T. Vink and G. G. P. Van Gorkom, *J. Lumin.* **5**, 379 (1972).
- <sup>17</sup>D. G. Andrianov, P. M. Grinshtein, G. K. Ippolitova, E. M. Omel'yanovskü, N. I. Suchkova, and V. I. Fistul, *Fiz. Tekh. Poluprovodn.* **10**, 1173 (1976) [*Sov. Phys.—Semicond.* **10**, 696 (1976)].
- <sup>18</sup>J. M. Baranowski, J. W. Allen, and G. L. Pearson, *Phys. Rev.* **167**, 758 (1968).
- <sup>19</sup>H. A. Weakliem, *J. Chem. Phys.* **36**, 2117 (1962).
- <sup>20</sup>B. N. Figgis, *Introduction to Ligand Field* (Wiley, New York, 1967).
- <sup>21</sup>(a) A. Fazzio and J. R. Leite, *Phys. Rev. B* **21**, 4710 (1980); (b) A. Fazzio and A. Dal Pino, Jr., *Rev. Bras. Fis. Semiconductors*, 436 (1983) (special issue).
- <sup>22</sup>L. A. Hemstreet, *Phys. Rev. B* **15**, 834 (1977).
- <sup>23</sup>L. A. Hemstreet and J. P. Dimmock, *Phys. Rev. B* **20**, 1527 (1979).
- <sup>24</sup>B. G. Cartling, *J. Phys. C* **8**, 3171 (1975).
- <sup>25</sup>G. G. De Leo, G. D. Watkins, and W. B. Fowler, *Phys. Rev. B* **25**, 4962 (1982).
- <sup>26</sup>V. Singh, U. Lindefelt, and A. Zunger, *Bull. Am. Phys. Soc.* **28**, 288 (1983), and unpublished results.
- <sup>27</sup>A. Zunger and U. Lindefelt, *Phys. Rev. B* **26**, 5989 (1982).
- <sup>28</sup>A. Zunger, *Phys. Rev. B* **28**, 3628 (1983).
- <sup>29</sup>J. A. Majewski, *Phys. Status Solidi B* **108**, 663 (1981).
- <sup>30</sup>L. F. Mattheiss, *Phys. Rev. B* **5**, 306 (1972).
- <sup>31</sup>T. M. Wilson, *Int. J. Quantum Chem.* **3S**, 757 (1970).
- <sup>32</sup>B. H. Brandow, *Adv. Phys.* **26**, 651 (1977).
- <sup>33</sup>W. Hoogenstraten, *Phillips Res. Rep.* **13**, 515 (1958).
- <sup>34</sup>K. Kocot and J. M. Baranowski, *Phys. Status Solidi B* **59**, K11 (1973).
- <sup>35</sup>M. Godlewski and M. Kaminska, *J. Phys. C* **13**, 6537 (1980).
- <sup>36</sup>V. I. Sokolov, V. V. Chernyaev, M. V. Chukichev, Vu Zoan M'en, and V. S. Vavilov, *Fiz. Tverd. Tela (Leningrad)* **25**, 1585 (1983) [*Sov. Phys.—Solid State* **25**, 915 (1983)].
- <sup>37</sup>S. A. Abagyan, G. A. Ivanov, Yu. N. Kuznetsov, and Yu. A. Okunev, *Fiz. Tekh. Poluprovodn.* **8**, 1691 (1974) [*Sov. Phys.—Semicond.* **8**, 1096 (1975)].
- <sup>38</sup>D. Engemann and Th. Hornung, unpublished result, quoted in Ref. 1, p. 200.
- <sup>39</sup>S. A. Abagyan, G. A. Ivanov, G. A. Kovoleva, Yu. N. Kuznetsov, and Yu. A. Okunev, *Fiz. Tekh. Poluprovodn.* **9**, 369 (1972) [*Sov. Phys.—Semicond.* **9**, 243 (1975)].
- <sup>40</sup>(a) V. F. Materov and V. K. Sobolevskii, *Fiz. Tekh. Poluprovodn.* **13**, 1655 (1979) [*Sov. Phys.—Semicond.* **13**, 965 (1979)]; (b) X. Z. Yang, H. G. Grimmeiss, and L. Samuelson, *Solid State Commun.* **40**, 427 (1983).
- <sup>41</sup>D. M. Loeschner, J. W. Allen, and G. L. Pearson, *J. Phys. Soc. Jpn. Suppl.* **21**, 239, (1966).
- <sup>42</sup>S. A. Abagyan, G. A. Ivanov, and G. A. Koroleva, *Fiz. Tekh. Poluprovodn.* **10**, 1773 (1976) [*Sov. Phys.—Semicond.* **10**, 1056 (1976)].
- <sup>43</sup>(a) B. Clerjaud (private communication), and in *Proceedings of the Fourth Lund International Conference on Deep Level Impurities in Semiconductors, Hungary, 1983* (Hungarian Academy of Science, Budapest, 1983); (b) B. Clerjaud, F. Gendron, and C. Porte, *Appl. Phys. Lett.* **38**, 212 (1981).
- <sup>44</sup>D. J. Robbins, *J. Lumin.* **24/25**, 137 (1981).
- <sup>45</sup>K. Suto and J. Nishizawa, *J. Appl. Phys.* **43**, 2247 (1972).
- <sup>46</sup>J. M. Noras and J. W. Allen, *J. Phys. C* **13**, 3511 (1980).
- <sup>47</sup>J. S. Griffith, *The Theory of Transition Metal Ions* (Cambridge University Press, London, 1971).
- <sup>48</sup>S. Sugano, Y. Tanabe, and H. Kamimura, *Multiplets of Transition-Metal Ions in Crystals* (Academic, New York, 1970).
- <sup>49</sup>A. G. O'Neill and J. W. Allen, *Solid State Commun.* **46**, 833 (1983); in *Abstracts of the Fourth International Conference on Deep Level Impurities in Semiconductors (Eger, Hungary, 1983)* (Hungarian Academy of Science, Budapest, 1983), p. 129.
- <sup>50</sup>S. Koide and M. L. M. Pryce, *Philos. Mag.* **3**, 607 (1967).
- <sup>51</sup>C. J. Ballhausen, *Introduction to Ligand Field Theory*, (McGraw-Hill, New York, 1962).
- <sup>52</sup>S. W. Biernacki, *Phys. Status Solidi B* **118**, 525 (1983).
- <sup>53</sup>R. R. Sharma, M. H. A. Viccaro, and S. Sundaram, *Phys. Rev. B* **23**, 738 (1981).
- <sup>54</sup>H. Watanabe, *Operator Methods in Ligand Field Theory* (Prentice-Hall, Englewood Cliffs, N. J., 1966).
- <sup>55</sup>G. W. Rubloff, *Surf. Sci.* **132**, 268 (1983).
- <sup>56</sup>V. A. Singh, A. Zunger, and U. Lindefelt, *Phys. Rev. B* **27**, 1420 (1983); V. A. Singh, U. Lindefelt, and A. Zunger, *Phys. Rev. B* **27**, 4909 (1983).
- <sup>57</sup>H. G. Grimmeiss, E. Jánzén, and B. Skarstam, *J. Appl. Phys.* **51**, 4212 (1980); **51**, 3740 (1980); **51**, 6238 (1980).
- <sup>58</sup>G. A. Baraff and M. Schlüter, *Phys. Rev. B* **19**, 4965 (1979).
- <sup>59</sup>J. Bernholc, N. Lipari, and S. T. Pantelides, *Phys. Rev. B* **21**, 3545 (1980).
- <sup>60</sup>(a) G. B. Bachelet, M. Schlüter, and G. A. Baraff, *Phys. Rev. B* **27**, 2545 (1983); (b) N. P. Ll'in and V. F. Materov, *Fiz. Tekh. Poluprovodn.* **12**, 772 (1978) [*Sov. Phys.—Semicond.* **12**, 451 (1978)].
- <sup>61</sup>H. P. Hjalmarson, P. Vogl, D. J. Wolford, and J. D. Dow, *Phys. Rev. Lett.* **44**, 810 (1980).
- <sup>62</sup>J. R. Troxel and G. D. Watkins, *Phys. Rev. B* **22**, 921 (1980).
- <sup>63</sup>U. Lindefelt and A. Zunger, *Phys. Rev. B* **26**, 846 (1982).
- <sup>64</sup>A. Hennel, *J. Phys. C* **11**, L389 (1978).
- <sup>65</sup>G. A. Slack, F. S. Ham, and R. M. Chrenko, *Phys. Rev.* **152**, 376 (1966).
- <sup>66</sup>G. A. Slack, S. Roberts, and F. S. Ham, *Phys. Rev.* **155**, 170 (1967).
- <sup>67</sup>G. A. Slack and B. M. O'Meara, *Phys. Rev.* **163**, 335 (1967).
- <sup>68</sup>C. Blanchard and R. Parrot, *Solid State Commun.* **10**, 413 (1972).
- <sup>69</sup>(a) J. T. Vallin and G. D. Watkins, *Phys. Lett.* **37A**, 297 (1971); (b) *Phys. Rev. B* **9**, 2051 (1974).
- <sup>70</sup>U. Kaufmann, H. Ennen, J. Schneider, and R. Wörner, *Phys.*

- Rev. B 25, 5598 (1982).
- <sup>71</sup>M. S. Skolnic, P. J. Dean, M. J. Kane, Ch. Uehlein, D. J. Robbins, W. Hayes, B. Cockayne, and W. R. MacEwan, J. Phys. C 16, L775 (1983).
- <sup>72</sup>J. Weber, H. Ennen, U. Kaufmann, and J. Schneider, Phys. Rev. B 21, 2394 (1980).
- <sup>73</sup>G. A. Pratt and R. Coelho, Phys. Rev. 116, 281 (1959).
- <sup>74</sup>J. Johansen and V. Wahlgren, Mol. Phys. 33, 651 (1977).
- <sup>75</sup>P. S. Bagus and V. Wahlgren, Mol. Phys. 33, 641 (1977).
- <sup>76</sup>L. Pauling, *The Nature of the Chemical Bond* (Cornell University Press, Ithaca, New York, 1960).
- <sup>77</sup>R. D. Shannon, in *Structure and Bonding in Crystals*, edited by M. O'Keefe and A. Navrotsky (Academic, New York, 1980), p. 53.
- <sup>78</sup>J. E. Huheey, *Inorganic Chemistry* (Harper & Row, New York, 1976), p. 294.
- <sup>79</sup>P. George, and D. S. McClure, Prog. Inorg. Chem. 1, 381 (1959).
- <sup>80</sup>A. Zunger, in *Structure and Bonding in Crystals*, edited by M. O'Keefe and A. Navrotsky (Academic, New York, 1980), p. 73.
- <sup>81</sup>A. Zunger, Phys. Rev. Lett. 44, 582 (1980).
- <sup>82</sup>J. K. Burdett, G. D. Price, and S. L. Price, J. Am. Chem. Soc. 104, 92 (1982); Phys. Rev. B 24, 2903 (1981).
- <sup>83</sup>R. E. Watson and L. H. Bennett, in *Alloy Phase Diagrams*, edited by L. H. Bennett, T. B. Massalski, and B. C. Giessen (North-Holland, New York, 1983), p. 99.
- <sup>84</sup>E. S. Machlin and E. Loh, Phys. Rev. Lett. 45, 1642 (1980). Compare A. Zunger, Phys. Rev. Lett. 47, 1086 (1981).
- <sup>85</sup>Calculations (e.g., Refs. 21, 22, 25, and 27) indicate a weak (<10%) dependence of the localization parameters of the gap states on the charge state.
- <sup>86</sup>U. Kaufmann and J. Schneider, Solid State Commun. 25, 1113 (1978).
- <sup>87</sup>V. I. Kirillov, N. N. Pribylov, S. I. Rembeza, A. I. Spirin, and V. V. Teslenko, Fiz. Tekh. Poluprovodn. 17, 1149 (1983) [Sov. Phys.—Semicond. 17, 724 (1983)].
- <sup>88</sup>W. C. Holton, J. Schneider, and T. L. Estle, Phys. Rev. 133, A1638 (1964).
- <sup>89</sup>A. Fazzio, M. J. Caldas, and A. Zunger, Phys. Rev. B 29, 5999 (1984).
- <sup>90</sup>J. Jaffe and A. Zunger, Phys. Rev. B 29, 1882 (1984).
- <sup>91</sup>J. W. Allen, in *Proceedings of the 7th International Conference on the Physics of Semiconductors, Paris, 1964*, edited by M. Hulin (Academic, New York, 1964), p. 781.
- <sup>92</sup>M. Kaminska, J. M. Baranowski, S. M. Uba, and J. T. Vallin, J. Phys. C 12, 2197 (1979).
- <sup>93</sup>R. K. Watts, Phys. Rev. 188, 568 (1969).
- <sup>94</sup>T. Ziegler, A. Rauk, and E. J. Baerendo, Theor. Chim. Acta 43, 261 (1977).
- <sup>95</sup>U. von Barth, Phys. Rev. A 20, 1693 (1979).
- <sup>96</sup>O. Gunnarson and B. I. Lundquist, Phys. Rev. B 13, 4274 (1976); J. H. Wood, J. Phys. B 13, 1 (1980).